Tekniska Högskolan iLund
Avdelningen för Bärande Konstruktioner

Lund Institute of Technology
Department of Structural Engineering

Lund 1996

Rapport TVBK-5078

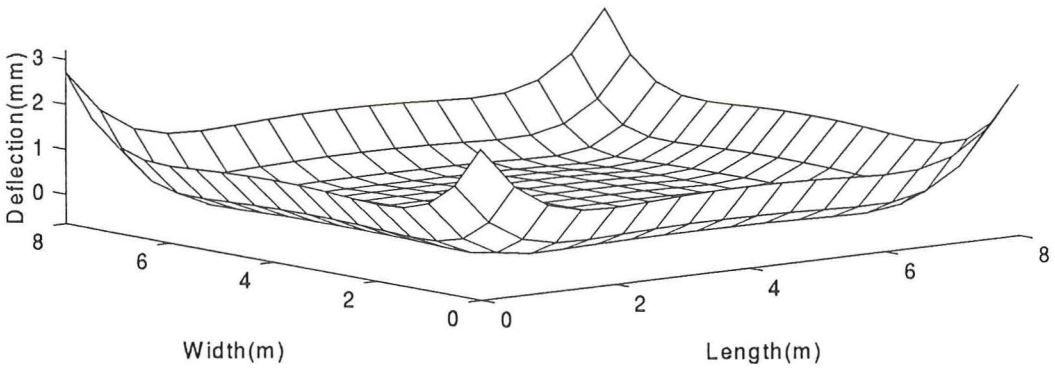

Design of Industrial Floors

Principles for Control of Warping

Mohammed Ali Alhasani and Ahmed Zaraei

Design of Industrial Floors

Principles for Control of Warping

Mohammed Ali Alhasani and Ahmed Zaraei

Rapport TVBK-5078
ISSN 0349-4969
ISRN: LUTVDG/TVBK--5078--SE

Examensarbete

Handledare: Sven Thelandersson

Januari 1996

Contents

Preface

The study presented in this Master's Thesis has been carried out at the Division of Structural Engineering, Lund Institute of Technology. It was carried out at the request of SKANSKA TEKNIK AB, Malmö.

The aim of this study is to assess the significance of the parameters involved in the serviceability of industrial floors, especially those concerning shrinkage. The analysis of industrial floor slabs is made using a finite element computer program, and the results of which are used to develop design principles for this kind of slabs.

We are most grateful to our supervisor, Professor Sven Thelandersson, for his guidance, and support during the course of this work. We wish also to thank Mr. Karl Gunnar Olsson, Lecturer, and Mr. Per-Erik Austrell, doctoral student; both at the Department of Structural Mechanics; for their valuable help during the early stages of the work.

Lund, December 1995

M. A. Alhasani, and A. Zaraei

Notation

A_s, A'_s	lower, and upper steel reinforcement
α	coefficient of thermal contraction of concrete
β	$= I_e / I_g$
b	width of concrete section, 1.0 m in case of slabs
c.g.	center of gravity
d	effective depth of flexural members
d´	distance from extreme fiber to compression reinforcement
δ	subgrade settlement
$\Delta\varepsilon_{sh}$	$= \varepsilon_{sht} - \varepsilon_{shb}$
ΔT	total equivalent temperature gradient, T_{egr} h, deg. C
e, e´	eccentricity of upper, and lower steel
E	modulus of elasticity of concrete
E_c	modulus of elasticity of concrete (short duration loading)
E_{ct}	sustained modulus of elasticity of concrete (long duration loading including creep effects)
E_{st}	modulus of elasticity of steel
E_r	$= E \beta$, reduced modulus of elasticity of concrete
ETG	equivalent temperature gradient
ε, ε'	shrinkage strain at upper, and lower steel levels
ε_{NA}	shrinkage strain at neutral axis
ε_{sht}	shrinkage strain at top surface of slab
ε_{shb}	shrinkage strain at bottom surface of slab
f_{ct}	tension strength of concrete
f_e	$= f_r - f_{res}$, effective modulus of rupture of concrete
f_{res}	restraint stress
f_s	allowable stress of steel reinforcement
F	auxiliary compression force in lower steel due to shrinkage, or coefficient of subgrade friction
F´	auxiliary compression force in upper steel due to shrinkage
ϕ	curvature of concrete member, M/E_cI
ϕ_0	initial curvature of plain concrete
ϕ_{cons}	curvature of reinforced concrete due to symmetrical shrinkage strain
ϕ_{vc}	curvature of plain concrete due to differential shrinkage strain
ϕ_{sv}	curvature of reinforced concrete due to differential shrinkage strain
γ	ratio between symmetrical shrinkage strain and the maximum value of differential shrinkage strain
h	slab thickness
I	moment of inertia
I_{cr}	moment of inertia of cracked transformed section
I_e	effective moment of inertia
I_g	moment of inertia of gross concrete section, neglecting reinforcement
k_s	modulus of subgrade reaction, N/m^3

K_{ss}	soil spring Contributing area * ks, N/m,
L	length of slab (or even width)
M	moment, Nm/m
M_a	maximum service load moment
M_{cr}	cracking moment
M_x	moment in slab around y-axis
M_y	moment in slab around x-axis
ν	Poisson's ratio
NA	neutral axis
p, p´	percentage of lower, and upper reinforcement's area to that of effective concrete area, = $100.A_s / bd$, and $100. A'_s / bd$
q	uniformly distributed load
t	time, and thickness of slab
T_{egr}, T_e	the equivalent temperature gradient, deg C/cm
w	weight of slab per unit area

1

Introduction

1.1 General remarks

The Slab-on-grade, which include Industrial floors, can be defined, according to ACI Committee 360,[1] as a slab continuously supported by ground with an area of more than twice the area required to support the imposed loads. The slab may be plain or reinforced and may include stiffening elements such as ribs and hidden beams. The reinforcement may be provided for structural purpose or for the control of effects of shrinkage and temperature changes.

Floor slabs are very important elements of industrial facilities. The slab must be uniformly flat and joints must be relatively level without excessive movements to allow manufacturing equipment and fork trucks to perform properly.

The development in industry has called for the use of bigger and heavier equipment and storage facilities. In addition, the development in construction practices such as the tendency to cast larger floor slabs with less joints, the use of high early strength cements, and the increase in using more admixtures has all led to the increase of cracking and curling of these slabs.

The way the uniform loads are stacked in warehouses are responsible for some cracking in the aisles between the loaded areas. The typical cracking in aisles consist mainly of two types. One type is longitudinal and the other is transverse. The cause of transverse cracking can directly be linked to shrinkage; while the cause of the longitudinal cracking is the way the external loading is stacked in warehouses. In warehouses, heavy uniform loads are normally distributed over partial areas of the slab, often around the columns leaving clear aisles midway between these columns. Commonly, the distance between the columns is such that the construction joints are located on column lines only. As shown in fig. 1.1.1, this will create a situation where longitudinal cracks appear

along the aisles, and as wheel loads pass over the cracked spots, secondary corner cracks appear.

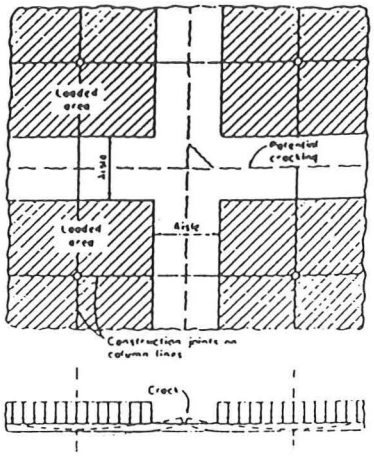

Fig. 1.1.1 — Potential cracking along the aisles. From Winter, et al.[2]

In addition to these two types of cracking, another type can be directly linked to shrinkage of floor slabs. This type of cracking occur: (1) near the perimeter of the contact area of warped slabs as the warped portion of the slab adjacent to the joints become unsupported by the ground and tend to break under the load, and (2) general cracking due to the restraint of shrinkage strain provided by the lower half of the slab.

Many measures has been proposed by different studies to control warping and cracking in floor slabs, or to enhance slabs ability to withstand their damaging effects. Control of cracking is achieved commonly by measures like supplementary reinforcement, proper design of joints, and the use of expansive cement, etc. All these measures are also helpful in controlling warping. The use of supplementary reinforcement for the sole purpose of reducing warping was suggested by some like Abdul-Wahab and Jaffer[3]. This approach was extensively studied and evaluated in the current study.

It should be noted that in the course of this study, the two expressions curling and warping will be used interchangeably.

1.2 Scope of this study

The purpose of this study is to investigate the phenomenon of warping and cracking of industrial floors. The use of supplementary reinforcement to control warping is evaluated, and the impact of many other factors on the magnitude of warping is studied.

The focus of the first part of this work will be on the development of a proper finite element model to analyze shrinkage and warping in industrial floor slabs. Later, design principles will be developed to benefit from the analysis results, and from the assessment of shrinkage parameters in floor slabs.

Although most of the shrinkage parameters change with time, the analysis will be implemented to space only.

1.3 The contents of this report

Chapter (2) gives the background to the problem of warping of slabs on grade. It includes a brief review of the past and present practices and theories.

Chapter (3) presents the theory behind warping of slabs-on-grade and the parameters affecting it. It also presents the finite element modeling of the problem and the computer program used for analysis.

Chapter (4) reviews the results of the parametric analysis of slabs on grade. The use of reinforcement to control warping in floor slabs is also evaluated.

Chapter (5) briefly reviews the design requirements to control shrinkage effects in industrial floor slabs.

Chapter (6) gives the concluding remarks.

2

Background

2.1 Warping of slabs-on-grade

2.1.1 The moisture gradient

Warping or curling of Slab-on-Grade is caused by differential changes in temperature and/or moisture content across the depth of the slab. These changes cause different length changes across the depth forcing the slab to curl up or down.

Upward curling is caused by the presence of a negative gradient, which is created when the moisture content, or temperature, at the top surface of the slab is less than at the bottom surface; while downward curling is caused by the presence of a positive gradient which is created when the moisture content, or temperature, at the bottom surface of the slab is less than at the top surface.

In slabs-on-grade, the moisture gradient is always negative, because, the slab's top dries much faster than its bottom, causing upward warping. If the slab is heated at the top surface, for instance by the sun, a positive temperature gradient is created causing the existing upward warping to decrease, or even to reverse, see fig. 2.1.1.

The moisture gradient depends on ambient humidity, concrete free water content, moisture content of the subgrade, and degree of freedom of movement of moisture between the slab and the subgrade. Measuring the resulting moisture gradient, therefore, is complex; while measuring the temperature gradient is much more easier. It is therefore more convenient to introduce the equivalent temperature gradient (ETG) to express the moisture gradient, or the accumulated effect of both moisture and temperature gradient. The units of (ETG) are deg C/cm of slab thickness.

Leonards and Harr[4] found that typical moisture gradients expressed as equivalent temperature gradient for enclosed floor slabs, is between 0.66 and 1.31 deg C/cm. In this study, the basic value of the equivalent temperature gradient is 1.3 deg C/cm.

At early ages, warping may be caused by heat of hydration of cement, especially in high cement content slabs. Heat of hydration accumulate at the bottom of the slab, causing the bottom to expand more than the top; hence, creating an early upward warping.

2.1.2 Enclosed versus external floor slabs

Warping of industrial floors is a typical form of warping of enclosed slabs-on-grade. Industrial premises are generally sealed from the effects of outside environment, and the temperature is generally constant. As the heating effect of the sun is excluded; the moisture gradient becomes the only source of warping. Therefore, warping of industrial floors is always upward.

It should be noted that, in Industrial premises the temperature at the top surface of the slab is higher than that at the bottom; hence, causing some downward warping. However, the amount of this downward warping is much less than the upward warping due to moisture gradient; and therefore, can not change the nature of warping in Industrial floors.

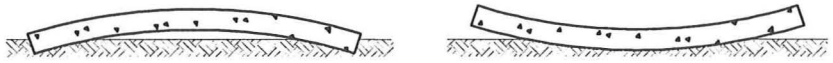

(a) (b)

Fig. 2.1.1— (a) Highway slabs curl down when the sun heats the slab (b) Enclosed slabs curl only upward.

2.1.3 Shape of slab curling.

It has been suggested by many that slabs curl in the shape of a circular arc, see for instance the argument of Ytterberg[5] regarding such statement in ACI's Concrete Craftsman Series: Slabs on Grade. This implies that vertical uplift at the slab edge increases with the square root of the distance between the joints. However, slabs on grade do not curl upward in the shape of a circular arc, because the weight of the slab prevents this. In addition, the vertical displacement at the slab edges does not increase as slab length increases beyond a certain length called the critical length, see chapter 4.

2.1.4 Warping stresses

When shrinkage strain is restrained, tensile stresses develop in the member, and often lead to cracking. In floor slabs, the restraint is provided by the lower part of the slab

which suffers less shrinkage than the top part. The lower part of the slab is also restrained by the friction between the slab and the subgrade. Therefore, tension stresses develop at the upper part with the possibility of causing cracks at the top surface wherever the restraint cause stresses greater than the tensile strength.

Curling commonly decreases with time, as moisture contents and temperatures equalize throughout the slab, reducing the equivalent temperature gradient. Creep also reduces curling after some period, see Sec. 3.2.

2.2 Historical Background

The attempt to develop a design method for the slab on grade first began at the beginning of this century. Early studies aimed at solving the design problems of highway and airport pavements. As early as 1910, several government agencies in USA conducted some field and laboratory tests to study the effects of environment conditions surrounding the concrete pavements. Those tests resulted among other things in 1922 in the discovery of the existence of a temperature gradient between the upper and lower surfaces of the pavement and the subsequent warping of the pavement slabs.

Meanwhile, other researchers has tried to develop the theory of the slabs on grade. Many proposals were made with the first one being filed in 1919 by A. T. Goldbeck as the "corner formula" to account for the weak subgrade under the corners. This proposal was later developed by Older in 1924 to a semi-empirical formula for the design of slab thickness on the assumption that the corners are unsupported by the ground. The field tests conducted then revealed a reasonable agreement between the corner formula and reality; yet, the use of this formula remained limited.

Between 1926-1927, Westergaard developed the first rigorous theoretical analysis of the structural behavior of concrete slab on grade. This theory considers an isotropic, elastic slab resting on an ideal subgrade known as the Winkler foundation that behaves like an infinite number of individual elastic springs. Westergaard analysis even considers the effects of thermal gradients, but stopped short of considering the effects of slab edges being unsupported by the ground.

Later, in 1930s, field observations and experiments showed good agreement between values measured in reality and values predicted by Westergaard as long as the slab remained in full contact with ground.

During this period, studies showed that many types of subgrade soils behave very close to an elastic, isotropic solid. Based on such type of subgrade, Burmister introduced the layered solid theory for the design of pavement slabs. He assumed that the slab is infinitely extent but finitely thick. The lack of solution to corners and edges of finite slabs meant that this theory has a very limited use in practice. Later, other theories based on the elastic, isotropic soil concept were developed, and a theory based on the yield-line concept also was proposed by Losberg.

In short, all design methods for the slab on grade can be grouped according to the type of model chosen to simulate the behavior of concrete and subgrade. There are three

models for the slab: (1) Elastic, isotropic solid, (2) Thin elastic slab, and (3) Thin elastic-plastic slab; and two models for the subgrade: (1) The Winkler type foundation, and (2) The elastic, isotropic solid. The existing design methods are based on different combinations of these models.

Since the introduction of the finite element method, the possibilities for analyzing slabs on grade has been greatly improved. Various models for slabs on grade has been proposed using finite elements like elastic blocks, rigid blocks, and torsion bars to represent the slab. The soil reaction is often modeled by uncoupled linear springs to simulate the Winkler foundation, or by some other arrangement of coupled springs to simulate the elastic, isotropic solid subgrade. For more details of this, see chapter 3; and for more details of the historical background of floor slab design refer, for instance, to ACI Committee 360[1], Leonards[4], Ytterberg Part (I) [5], and Al-Nasra[15].

2.3 Types of floors

The term Slab-on-Grade covers all types of slabs resting on ground including industrial floors, residential slabs, airport and highway pavements, parking lot slabs, and many others. Principally, all these slabs are similar in nature despite the need to treat each one of them differently. This difference is due to the nature of loading imposed on these slabs, the conditions surrounding them, and the specific requirement of each slab. The selection of a particular design method should, therefore, be based on considering the factors involved in a specific situation.

2.4 Current design methods

The present design methods are based on various combinations of the different models for slab and subgrade. Design aids of most of the current design methods are graphical consisting of charts produced from solutions of the selected model.

Each design method contains a different set of criteria that controls the parameters of the slab, but all aim to minimize cracking and produce the required serviceability. However, most of them put greater emphasis on those aspects regarding the slab ability to curry loads, but pay less attention to slab's serviceability. The wide spread cracking and warping problems in floor slabs confirms this fact.

In the current design methods, the only provision against shrinkage in floor slabs is the demand to design spacing of the joints in correlation with the supplementary shrinkage reinforcement. The amount of this reinforcement is calculated by the so called. subgrade drag formula, see eq. 5.7.1. This measure is taken to offset cracking due to concrete shrinkage which is restraint by the friction between the slab and the subgrade. Such steel is commonly placed near the top surface of the slab where it partially helps a little in curbing warping. This contribution is limited due to the limited amount of steel.

3

Developing The Model

3.1 Volume changes in concrete

The major volume changes that may occur in concrete are caused by: (1) settlement of fresh concrete, (2) loading, (3)chemical reactions in concrete which yield products having a different volume than that of the original constituents, (4) Temperature changes, and (5) drying.

Settlement of fresh concrete is of no importance to warping of industrial floors, because the concrete is in plastic or semi-plastic state; therefore, no significant stresses are developed in the concrete. The effect of rapidly applied load is to produce deformations which are largely elastic, and therefore, irrelevant to this study.

Volume changes caused by chemical reactions in concrete are called "Autogenous volume changes", because they are self-produced by internal reaction processes in the concrete. Such type of shrinkage is of importance to the interior of mass concrete where little or no loss of water takes place. Troxell and Davis[7] mentioned that, the maximum autogenous shrinkage at age 5 years for a variety of conditions is only about one-fifth the shrinkage of an average concrete. The autogenous volume change takes place slowly, and generally are not large enough to be a significant factor in the performance of floor slabs.

Volume changes caused by temperature are negligible in the case of industrial floors, because the temperatures inside the industrial premises are almost constant. However, temperatures at the top surface of the industrial floors are higher than those at its lower surface, i.e., downward curling is induced. This downward curling reduces the upward curling caused by drying shrinkage but its effect is marginal, and is, therefore, neglected. That only leaves drying shrinkage as the main factor in our study.

3.2 Drying shrinkage

Since drying shrinkage is the main source of warping of industrial floors; it is important to predict the amount of shrinkage strain in these floors.

The parameters which decide the amount of warping in floor slabs are the magnitude of drying shrinkage, thermal contraction, and creep. The accumulated effect of these parameters is influenced by the histories of water content, temperature, and loading (imposed, in this case, by drying shrinkage); therefore, any attempt to predict the magnitude and time of the maximum warping must consider these histories.

Although it is beyond the scope of this study to consider such details, it is useful to review briefly the development of shrinkage in slabs on grade.

After the end of the curing period, water starts to evaporate from the top surface of the floor slab creating a moisture gradient between the top and bottom surfaces. This gradient causes differential shrinkage across the thickness which in turn results in warping. The magnitude of shrinkage strain, and consequently that of warping continues to increase with time as more water evaporates from the top surface and the interior of the slab. This increase in shrinkage strain develops slowly and can continue for years. Fig. 3.2.1 shows the effect of time on the gradient of shrinkage strain across the thickness of the slab. Although shrinkage gradient is curvilinear in reality; the gradient is assumed here to be linear. The same assumption applies to the moisture gradient, which is expressed as the equivalent temperature gradient.

At later ages, the bottom of the slab starts to loose moisture; hence, changing the shape of the shrinkage strain distribution, from triangle to a trapezoid, see fig. 3.2.2. This change creates a new component of shrinkage strain (ε_{shb}), which is constant across the depth of the slab.

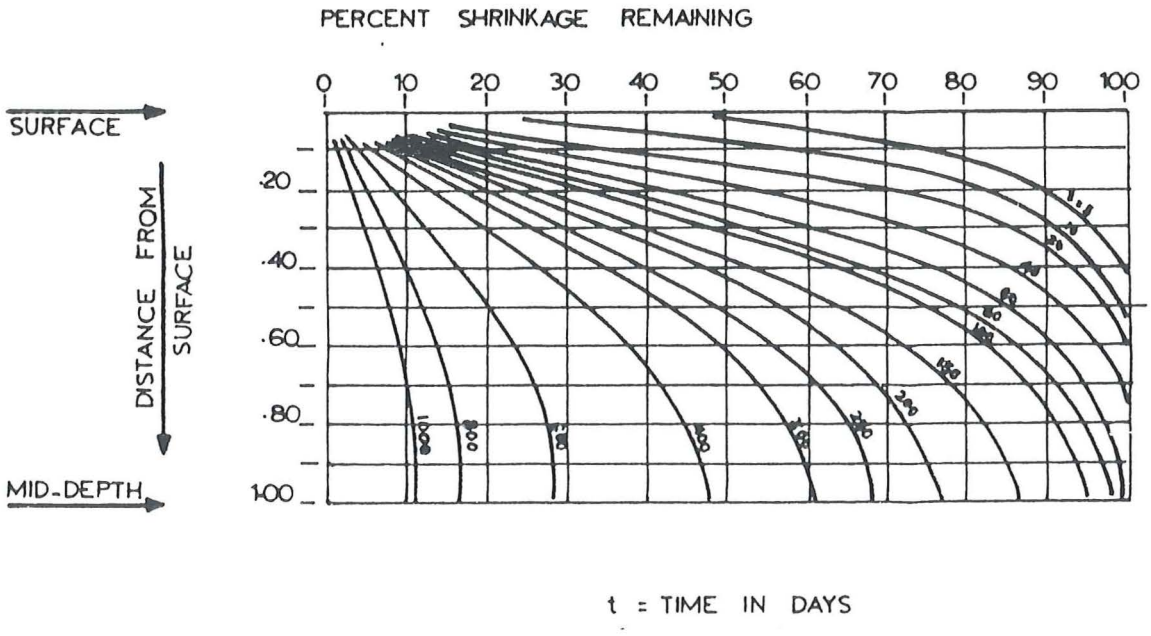

Fig. 3.2.1 — Development of shrinkage strain across the depth of a concrete member. Notice that (MID-DEPTH) represent floor's bottom surface. From Abdul-Wahab and Jaffer[3].

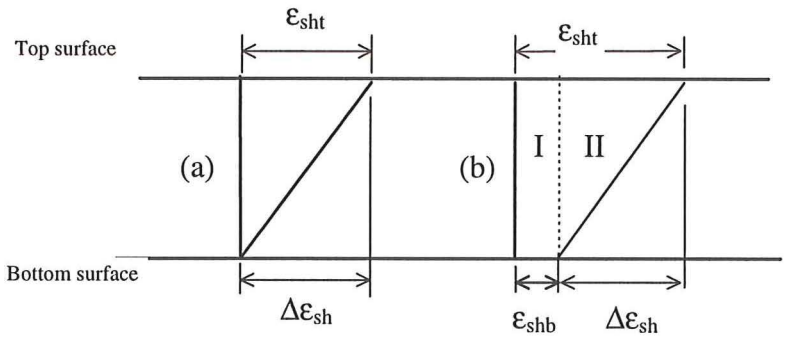

Fig. 3.2.2 — Dry shrinkage strain distribution, (a)before shrinkage in the bottom of the slab, and (b)after shrinkage in the bottom.

3.3 Shrinkage curvature

For convenience, the shrinkage strain distribution of fig. 3.2.2 (b) is divided into two components, (I) a symmetrical shrinkage, and (II) a differential shrinkage. In addition, a new variable (γ) is introduced, to represent the relationship between the magnitude of the shrinkage strain at the bottom , and that at the top, at any time (t). The new variable (γ), which will be used later in the computer program, is defined as

$$\gamma = \frac{\varepsilon_{shb}(t)}{\varepsilon_{sht}(t) - \varepsilon_{shb}(t)}\ 100 \qquad (3.3.1)$$

Where $\varepsilon_{sht}(t)$, and $\varepsilon_{shb}(t)$ are the shrinkage strains at time (t) at top-, and bottom surface respectively. $\Delta\varepsilon_{sh}$ is equal to

$$\Delta\varepsilon_{sh}(t) = T_{egr}(t).\ \text{slab thickness}\ .\ \alpha \qquad (3.3.2)$$

Where $T_{egr}(t)$. is the equivalent temperature gradient at time t, and α is the thermal contraction coefficient of concrete.

Each component of the shrinkage distribution affects warping of a concrete section in a different manner. Symmetrical drying shrinkage causes no curvature in a typical plain concrete section, but it does cause curvature in eccentrically reinforced concrete sections. However, this type of shrinkage is assumed to cause some curvature in plain concrete floor slabs due to restraint of movement by friction with the ground. The amount of such a curvature is minimal, and therefore, not included in this study.

The differential shrinkage, on the other hand, cause curvature in all types of concrete sections (plain, symmetrically-, and eccentrically reinforced sections).

Branson[8] and ACI Committee 209[9] reviewed some methods of computing shrinkage curvature due to symmetrical shrinkage in reinforced concrete members. They reviewed also a method of computing warping due to temperature changes in all types of concrete

members. In the current study, this method will form the basis of developing a method of computing shrinkage curvature due to differential shrinkage in plain concrete members; whereas, computing shrinkage curvature due to differential shrinkage in reinforced concrete will be based on the method developed by Abdul-Wahab and Jaffar[3]

3.3.1 Effect of the symmetrical shrinkage

Curvature (ϕ_c) due to symmetrical shrinkage strain in reinforced concrete sections is computed by eq. 3.3.3, and 3.3.4 which were proposed by Branson[8]

$$\phi_c = 0.7\,\frac{\varepsilon_{sh}}{h}(p-p')^{1/3}\sqrt{\frac{p-p'}{p}} \qquad \text{for } (p-p') \le 3.0\% \qquad (3.3.3)$$

$$\phi_c = \frac{\varepsilon_{sh}}{h} \qquad \text{for } (p-p') > 3.0\% \qquad (3.3.4)$$

Where $p = 100\,\dfrac{A_s}{bd}$ the percentage of the lower steel (3.3.5)

$p' = 100\,\dfrac{A'_s}{bd}$ the percentage of the upper steel (3.3.6)

$\varepsilon_{sh} = \varepsilon_{shb}$ symmetrical shrinkage (3.3.7)

$A_s,\ A'_s$ lower, and upper steel reinforcement

h slab thickness

The term (p - p′) must be positive; therefore, its absolute value is used in eq. 3.3.3, and the sign of curvature ϕ_c is changed accordingly.

3.3.2 Effect of differential shrinkage in plain concrete

Curvature (ϕ_{vc}) due to differential shrinkage in plain concrete is computed by eq. 3.3.10, which can be derived from fig. 3.3.1.

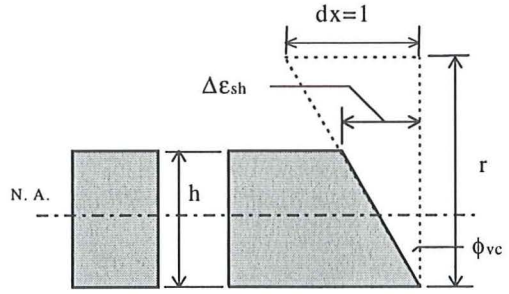

fig. 3.3.1 — Differential shrinkage of plain concrete section

$$\phi_{vc} = \frac{1}{r} = \frac{\Delta\varepsilon_{sh}}{h} \tag{3.3.8}$$

where $\Delta\varepsilon_{sh} = \Delta T\ \alpha = T_{egr}\ h\ \alpha$ (3.3.9)

i. e. $$\phi_{vc} = \frac{T_{egr}\ h\ \alpha}{h} = T_{egr}\ \alpha \tag{3.3.10}$$

and α is the coefficient of thermal contraction of concrete which is assumed to be constant and equal to 1.10^{-5} per deg C.

3.3.3 Effect of differential shrinkage in reinforced concrete

The method of computing curvature due to differential shrinkage in reinforced floor slabs is based on the method outlined by Abdul-Wahab and Jaffer.[3] Although their method was originally intended to compute the curvature of eccentrically reinforced concrete members drying from one face only, the method is readily applicable even to concrete members with similar reinforcement at top and bottom.

Fig. 3.3.2 illustrates a doubly reinforced concrete member subjected to differential shrinkage strain, i.e., shrinkage strain at the bottom is equal to zero. Considering the uncracked concrete section, shrinkage strain at the neutral axis is

$$\varepsilon_{NA} = \frac{\Delta\varepsilon_{sh}}{h} \cdot \frac{h}{2} = \frac{\Delta\varepsilon_{sh}}{2} \tag{3.3.11}$$

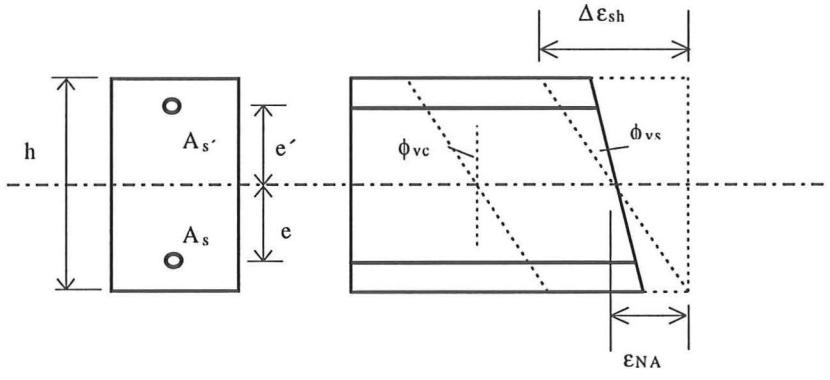

Fig. 3.3.2 — Differential shrinkage strain of reinforced concrete member

The initial shrinkage strain at the level of top, and bottom steel is

$$\varepsilon = \varepsilon_{NA} - e\,\phi_{vc} \qquad (3.3.12\ a)$$

and $$\varepsilon' = \varepsilon_{NA} + e'\,\phi_{vc} \qquad (3.3.12\ b)$$

Where (ϕ_{vc}) is given by eq. 3.3.8

The effect of reinforcement on curvature can be found by applying compressive forces to the steel. For bottom steel, the compressive force (F) is

$$F = \varepsilon\, E_s\, A_s \qquad (3.3.13\ a)$$

and for top steel

$$F' = \varepsilon'\, E_s\, A'_s \qquad (3.3.13\ b)$$

substituting eq. (3.3.12 a) and (3.3.12 b) into (3.3.13 a) and (3.3.13 b) respectively

$$F = (\varepsilon_{NA} - e\,\phi_{vc})\, E_s\, A_s \qquad (3.3.14\ a)$$

$$F' = (\varepsilon_{NA} + e'\,\phi_{vc})\, E_s\, A'_s \qquad (3.3.14\ b)$$

When these forces are released they are equivalent to tension loads at steel level. The forces (F), and (F′) are not equal; hence a bending moment is created

$$M = (\varepsilon_{NA} - e\,\phi_{vc})\, E_s\, A_s\, e - (\varepsilon_{NA} + e'\,\phi_{vc})\, E_s\, A'_s\, e' \qquad (3.3.15)$$

Curvature due to this moment is

$$\phi_{vs} = \frac{M}{(EI)_{eff}} \quad ; \text{where } (EI)_{eff} \text{ is the effective bending stiffness} \qquad (3.3.16)$$

i.e. $$\phi_{vs} = ((\varepsilon_{NA} - e\,\phi_{vc})\, E_s\, A_s\, e - (\varepsilon_{NA} + e'\,\phi_{vc})\, E_s\, A'_s\, e') / (EI)_{eff} \qquad (3.3.17)$$

Abdul-Wahab[3] confirmed experimentally a suggestion by Branson[8] that $(EI)_{eff}$ can be replaced by ($E_c\ I_g$ / 2), where (E_c) is the modulus of elasticity of concrete for short duration loading, and (I_g) is the moment of inertia of the gross concrete section; therefore, eq. (3.3.17) is modified to

$$\phi_{vs} = ((\varepsilon_{NA} - e\,\phi_{vc})\, E_s\, A_s\, e - (\varepsilon_{NA} + e'\,\phi_{vc})\, E_s\, A'_s\, e') / (0.5\, E_c\, I_g) \qquad (3.3.18)$$

3.3.4 Total Curvature

Curvature in floor slab (ϕ) due to both symmetrical-, and differential shrinkage is computed, by adding together the various curvature values

$$\phi = \phi_c + \phi_{vc} + \phi_{vs} \tag{3.3.19}$$

Equivalent moment due to curvature can then be computed by

$$M_i = \phi \, EI \tag{3.3.20}$$

3.4 Modulus of subgrade reaction

3.4.1 Model of the subgrade reaction

There are two models to simulate the behavior of subgrade reaction; the Winkler foundation and the elastic, isotropic solid. The Winkler foundation concept is based on the assumption that the soil behaves like an infinite number of individual elastic springs each of which is not affected by the others. The proportionality constant of these springs is the modulus of subgrade reaction (k_s), and is equal to the unit pressure required to produce a unit settlement. This concept may be compared to a slab resting on a dense liquid whose unit weight is equal to the modulus of subgrade reaction. The Winkler foundation is very easy to model. It can be modeled as a slab supported by uncoupled springs as illustrated in fig. 3.4.1 (b) . The modulus of subgrade reaction is defined by the equation:

$$k_s = q / \delta \tag{3.4.1}$$

Where (q) is the load per unit area exerted on the subgrade, and (δ) is slab's downward deformation.

When the Finite Element Method is implemented to analyze the floor, the effect of soil reaction is accumulated at the grid nodes by multiplying the modulus of subgrade reaction by the contributing area for each node. The result of this product, which is normally called the soil spring, is applied to that node. The proportionality constant of the soil spring (K_{ss}) has the units of a spring, i.e., N/m, and is defined by

$$K_{ss} = \text{Contributing area} \; . \; k_s \tag{3.4.2}$$

The other foundation model is the elastic, isotropic solid as in the Boussinesq theory. This type of foundation is modeled by coupling the subgrade springs as illustrated in fig. 3.4.1 (a). By coupling, the system equation become much more complicated than in uncoupled springs, but also give more accurate results.

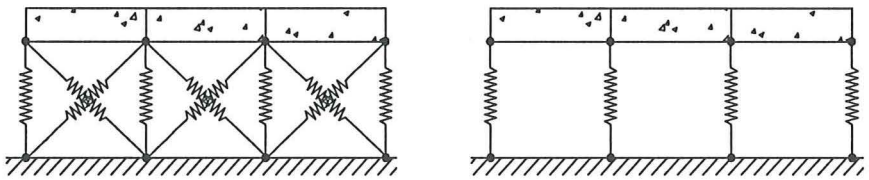

(a) (b)

Fig. 3.4.1 — (a) Coupled-, and (b) uncoupled soil spring models.

Values of the modulus of subgrade reaction (k_s) can only be approximate, because the value changes with many factors like: depth of soil layers, variation in soil properties from point to point under the same structure, and time, etc. The methods used to evaluate k_s which are based on Terzaghi's rules also contributes to the uncertainty of estimating k_s values.

Therefore, it is more practicable to adopt a simple subgrade model; namely, the uncoupled system. However, it is still possible to adopt a simple and more accurate method based on the Boussinesq theory, i.e., with coupling. ACI Committee 336[11] outlined a method which indirectly allows for coupling effect by reducing spring stiffness for the slab's interior. This method relies on the Boussinesq theory and will generally be adequate if some additional computational refinement is required. It is the most accurate of the approximate methods, but is also more difficult. ACI Committee 336[11], Bowels[12], and Shukla[13] proposed a much simpler procedure which tends towards getting the same effect of coupling, but very easy to program by simply doubling the stiffness of end node springs. This procedure is adopted in the current study.

The obvious effect of coupling vs. uncoupling is that coupling of soil springs produce a more realistic dish-like settlement profile beneath a uniformly loaded structure, while uncoupled springs produce a constant settlement profile.

3.4.2 The gap-spring

The soil springs used in this study are of the so called gap-spring type, which simulate a compression-only foundation. The subgrade only resists pressure exerted by the floor slab when it moves down, and offers no resistance to tension when the slab moves up. Fig. 3.4.2 illustrates the Gap-spring, which is a typical spring with additional gap plates. The downward movement of the slab will press the plates together; thus conveying the

force through the spring to the subgrade. When the slab moves up, the plates separate, and resistance to movement is eliminated.

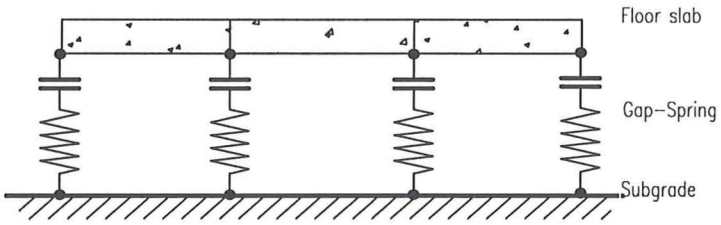

fig. 3.4.2 - The gap-spring.

3.5 Finite Element Modeling

3.5.1 General

As was explained in sec. 3.1 above; predicting the magnitude of maximum equivalent temperature gradient, expected to take place in floor slabs, must consider the combined effects of the temperature, moisture, and creep. The method required to solve such type of a problem is one of employing the finite element method both to space and time taking into consideration the relevant material properties.

In the current study, finite element method is employed only to space to analyze the floor slab at a certain time. The concrete floor slab is represented by four-node rectangular plate elements, and the soil reaction is represented by spring elements of the gap-spring type. These springs are applied at the grid nodes, and have stiffness equal to K_{ss}. Fig. 3.5.1 illustrates the plate element, and the springs attached to it.

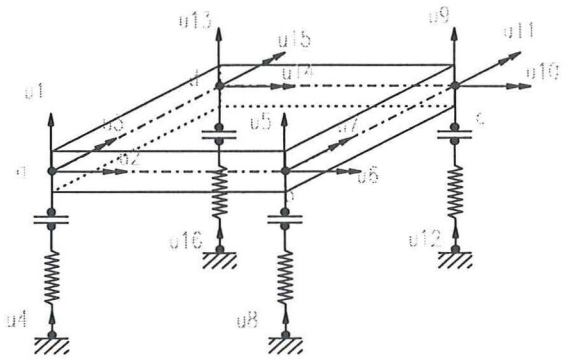

Fig. 3.5.1 — Plate element with the soil springs

Slab edges are assumed to be free with no external restraint except the friction with the ground. This friction is not considered in the current study.

3.5.2 Material Model

Plane stress constitutive relation was assumed and the slab material is assumed to be linear elastic isotropic. The stress-strain relation for such material is

$$\begin{bmatrix} \sigma_x \\ \sigma_y \\ \tau_{xy} \end{bmatrix} = \frac{E}{1-\nu^2} \begin{bmatrix} 1 & \nu & 0 \\ \nu & 1 & 0 \\ 0 & 0 & \frac{1}{2}(1-\nu) \end{bmatrix} \begin{bmatrix} \varepsilon_x \\ \varepsilon_y \\ \gamma_{xy} \end{bmatrix} \tag{3.5.1}$$

Which can be written in matrix form as

$$\boldsymbol{\sigma} = \mathbf{D}\,\boldsymbol{\varepsilon} \tag{3.5.2}$$

To include the initial shrinkage strain ε_0, eq. 3.5.2 is replaced by

$$\boldsymbol{\sigma} = \mathbf{D}\,\boldsymbol{\varepsilon} - \mathbf{D}\,\boldsymbol{\varepsilon}_0 \tag{3.5.3}$$

For simplicity, the constitutive relation will be considered in the form given by eq. 3.5.2. The moment curvature relationships is obtained by

$$\begin{bmatrix} M_x \\ M_y \\ M_{xy} \end{bmatrix} = \frac{E\,t^3}{12(1-\nu^2)} \begin{bmatrix} 1 & \nu & 0 \\ \nu & 1 & 0 \\ 0 & 0 & \frac{1}{2}(1-\nu) \end{bmatrix} \begin{bmatrix} \phi_x \\ \phi_y \\ \phi_{xy} \end{bmatrix} \tag{3.5.4}$$

And in matrix-form as

$$\mathbf{M} = \tilde{\mathbf{D}}\,\boldsymbol{\Phi} \tag{3.5.5}$$

where $\tilde{\mathbf{D}} = \frac{t^3}{12}\,\mathbf{D}$ and t is the slab thickness (3.5.6)

and $$\boldsymbol{\Phi} = \begin{bmatrix} \phi_x \\ \phi_y \\ \phi_{xy} \end{bmatrix} = \begin{bmatrix} \frac{\partial^2 \omega}{\partial x^2} \\ \frac{\partial^2 \omega}{\partial y^2} \\ 2\frac{\partial^2 \omega}{\partial x \partial y} \end{bmatrix} \tag{3.5.7}$$

3.5.3 System Stiffness Matrix

The stiffness matrix of the whole slab system is obtained by assembling the stiffness matrices of slab elements, and those springs under compression. The element stiffness of the slab is that of a typical four node rectangular plate element as defined in fig. 3.5.1, and the element stiffness of the subgrade is a typical 2x2 matrix of a spring having stiffness equal to K_{ss}. Spring stiffness of end nodes are doubled to create the coupling effect (see Sec. 3.4).

3.5.4 Equivalent load

The initial strain method is used to account for curling deformations. The restraining forces required to prevent deformations due to shrinkage are applied as equivalent loads to rotation degrees of freedom of the plate element on the whole floor slab.

For plane stress, the equivalent load moment caused by shrinkage around x-axis is given by

$$M^e_{ix} = - \phi_x E_x I_{ex} /(1-\nu) \tag{3.5.8}$$

and the equivalent load moment around y-axis

$$M^e_{iy} = - \phi_y E_y I_{ey} /(1-\nu) \tag{3.5.9}$$

Where

M^e_{ix}, M^e_{iy} the equivalent loads (moments) due to shrinkage,

ϕ_x , ϕ_y curvature due to shrinkage

E_x , E_y the modulus of elasticity of concrete (including the effects of cracking in case of State-II analysis)

I_{ex} , I_{ey} effective moment of inertia

The system equation is represented by

$$\mathbf{K} \,.\, \mathbf{a} = \mathbf{f} + \mathbf{f_0} \tag{3.5.10}$$

Where (**K**) is the system stiffness matrix, (**a**) is the displacement vector, (**f**) is the actual load including self weight and imposed loads, and ($\mathbf{f_0}$) is the system equivalent load vector which is obtained by assembling the element equivalent load vector ($\mathbf{f^e_0}$)

$$\mathbf{f}^e_0 = \begin{bmatrix} 0 & M^e_{ix} & -M^e_{iy} & 0 & M^e_{ix} & M^e_{iy} & 0 & -M^e_{ix} & M^e_{iy} & 0 & -M^e_{ix} & -M^e_{iy} \end{bmatrix}^T \tag{3.5.11}$$

3.5.5 Effective moment of inertia

The effective moment of inertia of cracked concrete section which accounts for the gradual transformation from the uncracked to the full cracked section is given by

$$I_e = \left(\frac{M_{cr}}{M_a}\right)^3 I_g + \left[1 - \left(\frac{M_{cr}}{M_a}\right)^3\right] I_{cr} \qquad (3.5.12)$$

Where M_{cr} is the cracking moment, M_a is the maximum moment, I_g is the moment of inertia of the gross section neglecting the steel, and I_{cr} is the moment of inertia of the cracked transformed section.

Eq. 3.5.12 is applied only when $M_a \geq M_{cr}$; otherwise, $I_e = I_g$. That means, I_e has upper and lower limits of I_g and I_{cr}, and thus, the equation accounts for the gradual transformation from uncracked to full cracked section. Cracking moment of the concrete section is given by

$$M_{cr} = \frac{f_r I_g}{y_t} \qquad (3.5.13)$$

Where (y_t) is half the depth of the concrete section.

Eq. 3.5.12 was first introduced by (Branson 1963) and later adopted by the 1971 ACI code. A single value of the effective moment of inertia is calculated by eq. 3.5.12 at the location of the greatest moment M_a. This single value is then adopted for the whole floor slab.

Since floor slabs are restraint against shrinkage; tensile stresses are developed in the member. Such tensile stresses develop over a rather long period of time so they are at least partially relieved by creep effects, but a certain amount of restraint stresses should be expected at early ages. Scanlon and Murray,[14] concluded that this argument should always be considered when calculating effective moment of inertia (I_e) for use in slab deflection calculations.

To account for the presence of restraint stresses, the modulus of rupture (f_r) is reduced by the amount of the restraint stress (f_{res}) to get the effective modulus of rupture. Restraint stress is either estimated, or calculated by multiplying the relevant strain by the modulus of elasticity of concrete. The effective modulus of rupture is given by

$$f_e = f_r - f_{res} \qquad (3.5.14)$$

So, eq. 3.5.13 is modified to account for restraint stresses

$$M_{cr} = \frac{f_e I_g}{y_t} \qquad (3.5.15)$$

Since the magnitude of the restraint stress (f_{res}) depends, among other things, on the magnitude and history of shrinkage strain which do not form a part of this study; (f_{res}) was assumed to have a constant value equal to (0.2 f_r), i.e.

$$f_e = 0.8\, f_r \tag{3.5.16}$$

3.5.6 Cracking Model

The use of a general purpose finite element computer program has promoted the use of the following procedure to include the effects of cracking in slabs.

The floor slab is first loaded with service loads including the equivalent loads of shrinkage. A linear analysis is performed on the uncracked slab under the action of the combined loads. Based on this analysis, M_x and M_y are calculated for each element. If the highest computed moment is greater than cracking moment, cracking occurs and flexural stiffness should be reduced.

The reduction in flexural stiffness is accomplished by reducing the moment of inertia. The reduced moment of inertia is called the effective moment of inertia (I_e), and is computed by eq. 3.5.12. Material properties are then modified by multiplying the modulus of elasticity of concrete by the reduction factor (β), to reflect the reduction in stiffness due to cracking

$$E_r = \beta\, E \tag{3.5.17}$$

where $$\beta = \frac{I_e}{I_g} \tag{3.5.18}$$

Analysis is then repeated using the reduced modulus of elasticity (E_r).

3.5.7 Change of boundary conditions

When the floor slab is loaded with the equivalent load of shrinkage, curling takes place lifting the slab in some areas of the ground. The soil springs at these areas become in tension, and are disconnected leaving the slab in partial contact with the ground; hence, changing the boundary conditions. A new analysis is then performed with the new boundary conditions. This process is repeated and the springs are disconnected or reconnected as required until the forces reach an equilibrium state.

3.5.8 Computer Program

The finite element computer program used in the analysis is based on the CALFEM program which has been developed at the Division of Structural Mechanics in Lund University. The CALFEM is an interactive computer program for teaching the finite element method. It has been developed as a toolbox to MATLAB, and can be used for different types of structural mechanics-, and field problems.

The CALFEM was used in the batch oriented mode; where sequence of functions are written in a so called .m file, and evaluated by writing the file name in the command window. The program was supplemented with the necessary subroutines and batch files to deal with the requirements of analyzing industrial floors.

The maximum number of plate elements used in the analysis was 16x16, because of the limited capacity of the personal computer used to carry out the analysis, resulting in setting a maximum limit on slab length (or width) to around 10-12 m in order to get a good computational accuracy.

The computer program conducts the following operations for a typical cycle of analysis

1. Collect input data
2. Calculate section properties like I_g , M_{cr} , etc.
3. Calculate system geometry matrices.
4. If analysis is done in State II; the effective moment of inertia and the reduced modulus of elasticity are calculated.
5. Compute slab element equivalent load vector.
6. Assemble global equivalent force vector ($\mathbf{f_e}$).
7. Calculate slab element load vector ($\mathbf{f_0^e}$).
8. Assemble global load vector ($\mathbf{f}$) .
9. Calculate slab element stiffness matrix($\mathbf{K_e}$).
10. Assemble global stiffness matrix ($\mathbf{K}$).
11. Solve the system equation.
12. Modify the stiffness of the springs: reduce the stiffness of those springs in tension to zero, and restore the stiffness of those springs which are again in compression. If all spring elements are in compression go to 14.
13. Go to 10.
14. Calculate element stresses.
15. Display the results in matrices and figures.

4

Analysis Results

4.1 Introduction

To study the response of slab of grade (SOG) towards variations in the different parameters; the slab is analyzed using various combinations of parametric values. The parameters in question are

- Equivalent temperature gradient (T_{egr}).
- Modulus of elasticity of concrete (E_c).
- Slab thickness (t).
- Modulus of subgrade reaction (k_s).
- Slab length, or width (L).
- Steel reinforcement (p, and p´).
- Time factor (γ).
- External loading.

The analysis is to be carried out in three phases. In the first one, a plain concrete SOG is analyzed to assess the significance of T_{egr} , E_c , k_s , t, and slab length. The second phase will deal with reinforced slab on grade. Here, the influence of various combinations of lower-, and upper steel reinforcement (p, and p´ respectively) will be assessed. The assessment will include the time factor (γ). The third phase will generally be the same as phase two with the addition of various external loads.

Regarding the results which are demonstrated in figures, and tables within the text and in the Appendix; one should only observe that

- The values of vertical deflection referred to in the tables and in some figures are those of the slab corner.

- The deflection is measured from the original zero level.
- Vertical deflection profiles, and moment diagrams are drawn along the diagonal of the slab.

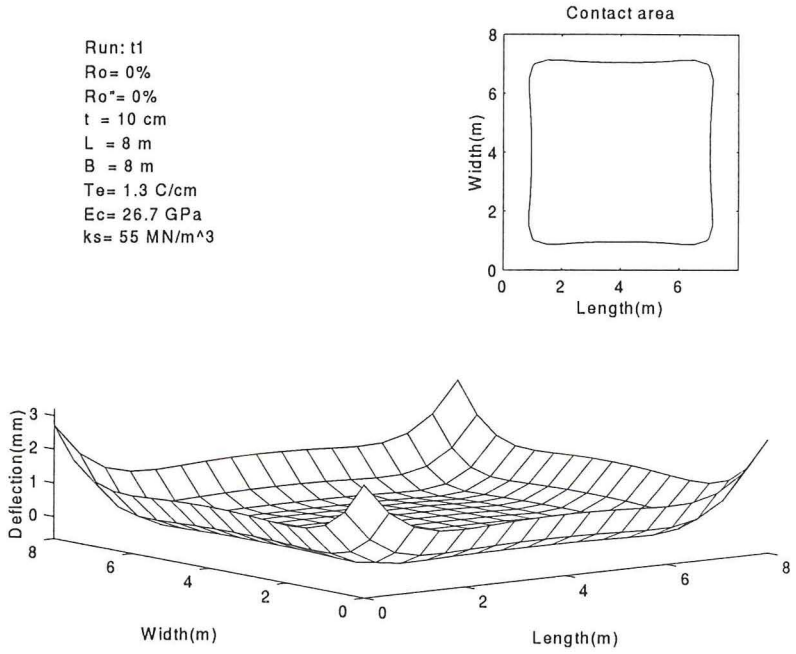

Fig. 4.1.1— A typical 3D representation, and the contact area of a warped slab.

4.2 Analysis of plain concrete slab

4.2.1 Assumptions and parameters

A plain concrete slab will be used to investigate the effect of T_{egr} , E_c , k_s , t, and slab length. The reference values of the these parameters are: T_{egr} = 1.3 deg C / cm, E_c = 25.0 GPa, k_s =55.0 MN / m^3, L = 6.1 m, and t = 150 mm.

Each set of analysis is done by varying the value of one parameter while keeping the others equal to the reference values. The results of these analyses are presented in figures 4.2.1-4.2.8 on the next page.

4.2.2 Effect of equivalent temperature gradient

The analysis is carried out using values of (T_{egr}) between 0, and 1.8 deg C / cm, and the results are presented in fig. 4.2.1, and 4.2.2. They indicate that as the value of (T_{egr}) increases, warping also increases and the contact area decreases. The highest moment value roughly follows the perimeter of the contact area, and it becomes larger as T_{egr} grows, because larger values of (T_{egr}) produce larger values of curvature.

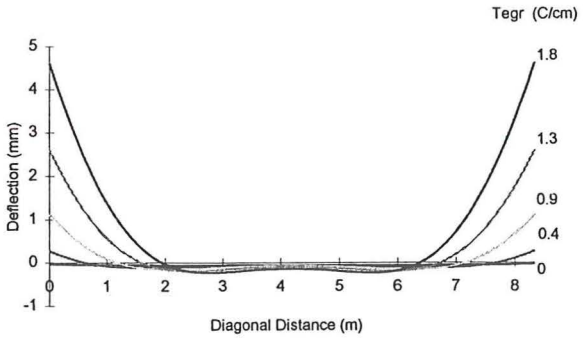

Fig. 4.2.1-- Effect of (T_{egr}) on slab warping.

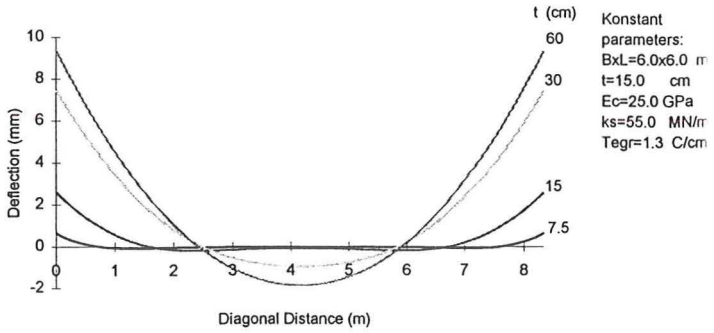

Fig. 4.2.3 -- Effect of (t) on slab warping.

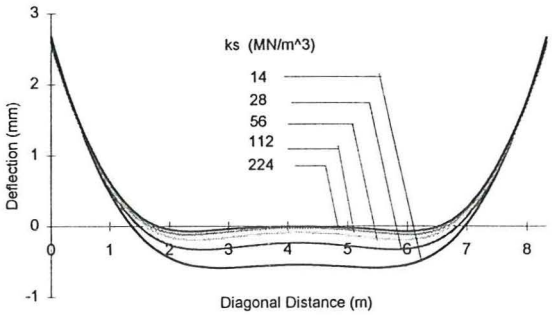

Fig. 4.2.5 -- Effect of (ks) on slab warping.

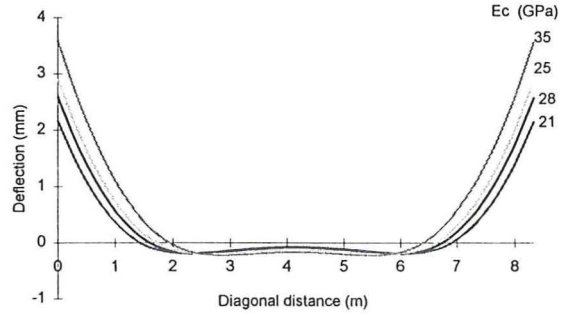

Fig. 4.2.7 -- Effect of (Ec) on slab warping.

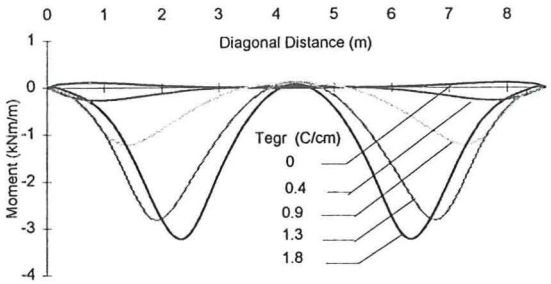

Fig 4.2.2 -- (Mx) - (Te) relation.

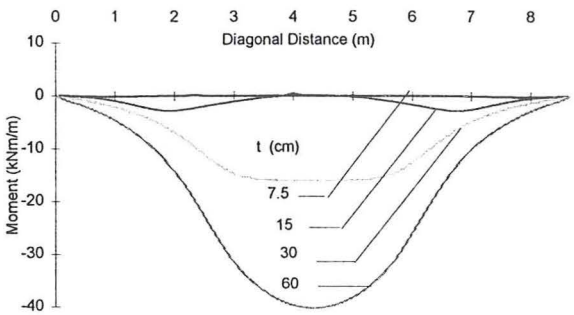

Fig. 4.2.4 -- (Mx) -(t) relation.

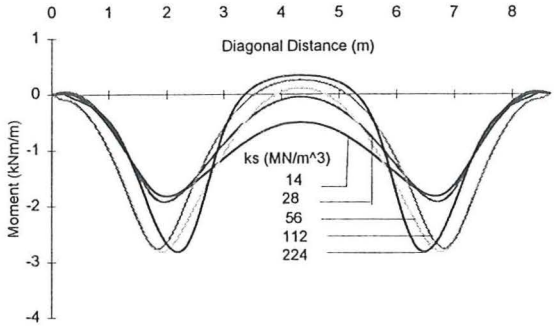

Fig. 4.2.6 -- (Mx) -(ks) relation.

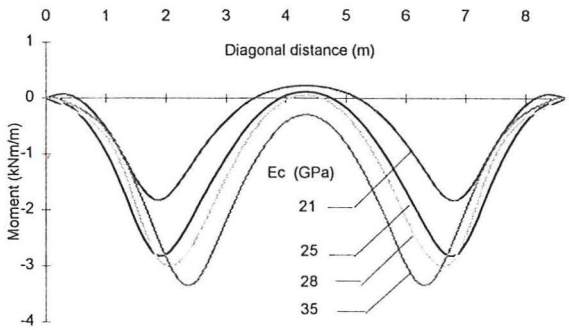

Fig.4.2.8 -- (Mx) -(Ec) relation.

4.2.3 Effect of slab thickness

The role of slab thickness (t) is rather complex, as variation in slab thickness produce different, and in many cases opposite, effects on warping. Weight of the slab depends on its thickness. Thick slabs are heavier than thin ones; therefore, they suffer less warping, because they resist warping uplift more efficiently, and sink deeper into the ground. On the other hand, greater thickness means higher curvature values, and stiffer slabs yielding higher initial moment, see eq. 3.5.8.

In addition, thickness affects the value of curvature itself. It influences also shrinkage development, and creep (due to variations in loading); hence, changing slab thickness changes the conditions which decide magnitude, and time at which maximum warping effect occur, see Sec. 3.2.

Such a problem can possibly be solved by the implementation of FEM analysis in both time and space. Although this kind of treatment is beyond the scope of this study, an attempt is made to investigate the implication of changing the thickness by adopting certain simplified conditions, which are: (1) Keeping (T_{egr}) constant, which means that the shrinkage strain at the top surface (ε_{sht}) becomes variable, or (2) Keeping (ε_{sht}) constant, which means that (T_{egr}) becomes variable.

Analysis result of these two cases are shown in fig. 4.2.3, 4.2.4, and 4.2.9 which show a clear difference between the two. For a constant (T_{egr}), the increase in thickness produces more warping in slab-on-grade, while for a constant (ε_{sht}), it produces less clear-cut change in warping.

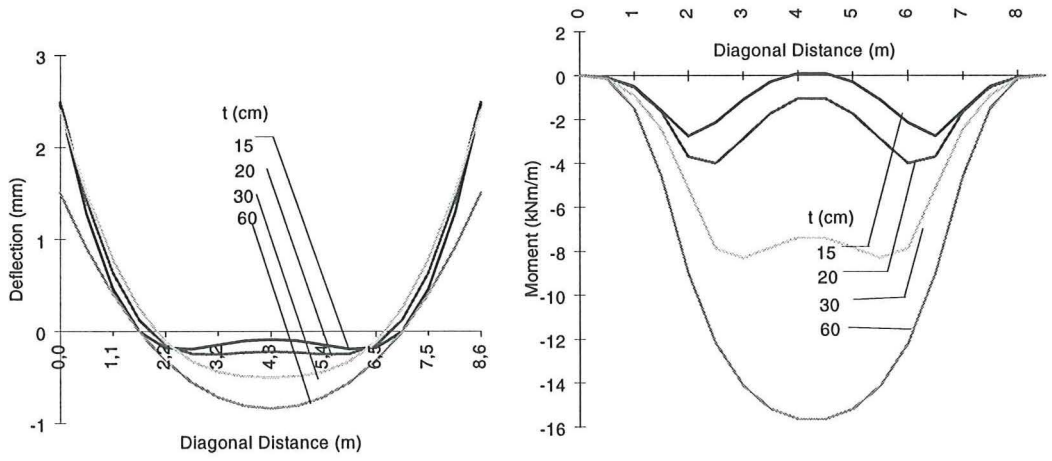

Fig. 4.2.9 — Deflection, and moment of SOG as a function of (t), with constant top fiber shrinkage strain, i.e. with variable (T_{egr}).

The reason for the results of the first case is understandable, because keeping (T_{egr}) constant while increasing the thickness results in greater shrinkage strain at the top fiber which result in greater curvature. On the other hand, the reason behind the results of the

second case is rather ambiguous. The inconsistency between the two results, which is even reflected in literature, may suggest the need for examining more closely the effect of changing slab thickness under constant environment condition.

4.2.4 Effect of modulus of subgrade reaction

Normally, the modulus of subgrade reaction (k_s) varies between 14 and 224 MN/m^3. This range of k_s represent the most common types of subgrade.

Figure 4.2.5, and 4.2.6 show that k_s value has a limited effect on slab deflection, and some effect on the moment.

The function of k_s is that it regulates the depth to which the slab sinks into the ground. When k_s increases, the subgrade become stiffer and slab sinks less into the ground forcing a greater portion of the slab to warp upwards; thus, increasing the moment. The corner deflection changes, otherwise, very little.

4.2.5 Effect of modulus of elasticity of concrete

The results of studies for E_c of 35, 28, 25, and 21 Gpa and their effect on the deflection along the slab diagonal are shown in fig. 4.2.7, and 4.2.8 which show that an increase in Ec increases warping deflection due to the increase in the applied equivalent moment. They show also that the contact area decreases forcing a greater portion of the slab to warp upwards; thus increasing the warping moment.

4.2.6 Critical slab length

The critical slab length (L_{cr}) is that length at which warping effect reaches its peak, and which vertical deflection and warping stresses remain basically constant.

Figure 4.2.10-4.2.13 show the influence of (t), (E_c), and (k_s) on the critical slab length. They show that, the critical length is only dependent on the thickness.

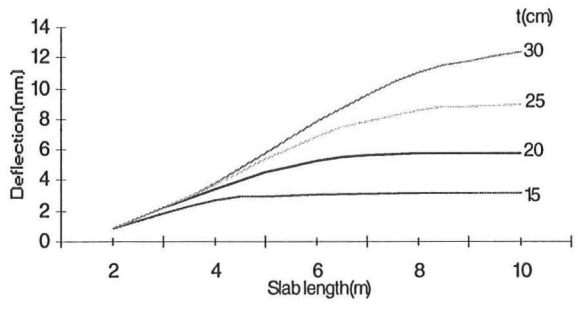

Fig. 4.2.10 — Slab length-Corner deflection relation for various (t).

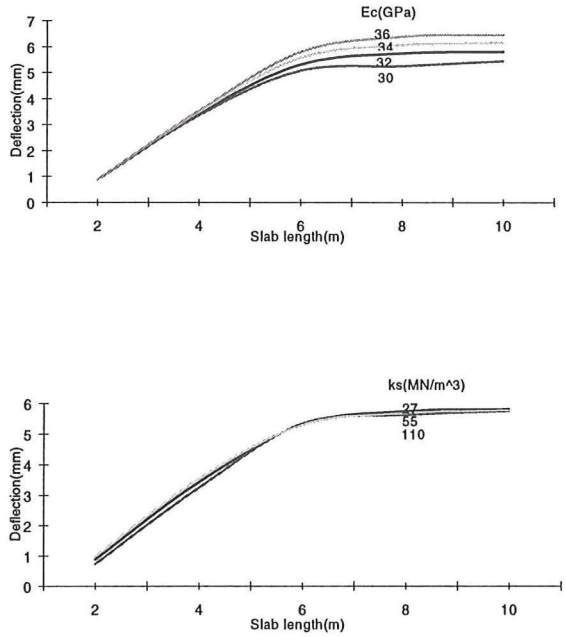

Fig. 4.2.11 — Slab length-Corner deflection relation for various values of E_c (above), and k_s (below)

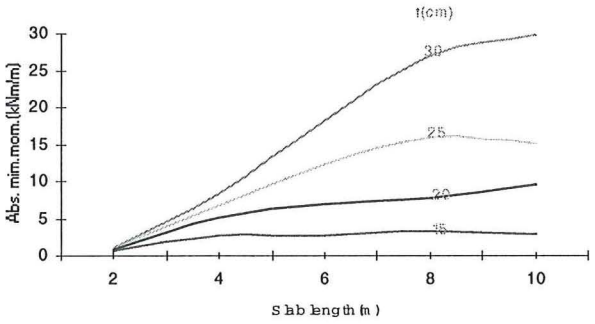

Fig. 4.2.12 — Warping moment as function of slab lengths, and thickness.

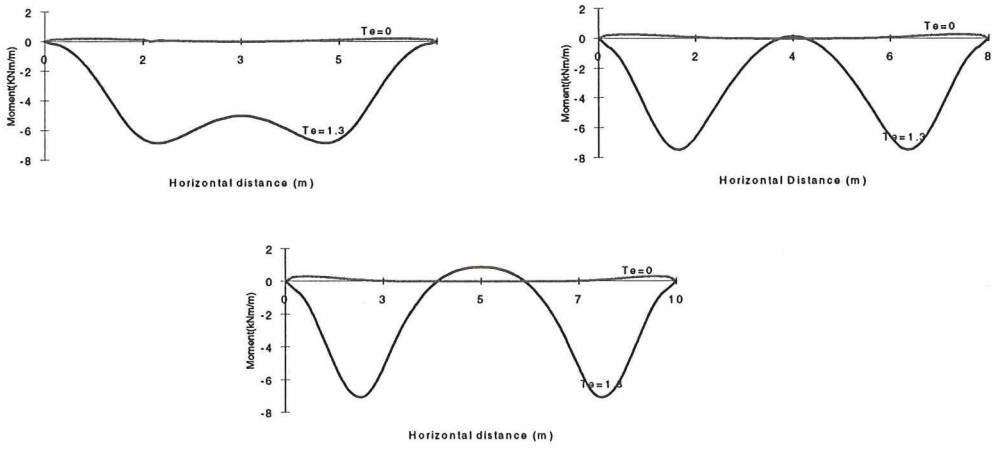

Fig. 4.2.13 — Moment diagram for different slab lengths, for T_{egr} = 0 deg C/cm (i.e., slab is only loaded with its own weight), and T_{egr} = 1.3 deg C/cm.

Figure 4.2.13 shows the moment diagrams for various slab lengths with all the other factors equal to the reference values. It shows that the highest moment remains almost constant for slab lengths greater than the critical slab length (here L_{cr} equals to 4.5 m, see fig. 4.2.10).

4.3 Effect of reinforcement

4.3.1 Assumptions and parameters

The effect of various percentages of reinforcement is studied using a 8.0x8.0 m slab. The values of k_s, and T_{egr} are kept equal to the reference values, i.e., k_s = 55.0 MN/m^3, and T_{egr} = 1.3 deg C/cm; while the other parameters are varied as following: t = 20.0, and 30.0 cm; E_c =32.0, and 34.0 Gpa (representing concrete types K40, and K50; according to BBK 94[20]). The time factor is included in the analysis by using different values of the coefficient (γ), see eq. 3.3.1. The value of (γ) is equal to 30, 60, and 90 %, resembling an early, middle, and old age shrinkage respectively.

The percentage of tension (lower) steel in slabs-on-grade normally ranges between 0.0 - 0.5 %. This range is adopted as the basic value for the lower steel (p), while for the upper steel, much less (p´) values are normally used for the control of shrinkage cracking. The approach adopted in this study is to use much higher (p) to reduce warping in the slab. The adopted range of (p´) is between 0.25-1.5 %. The 0 % value is not used, as the effect of having no upper reinforcement is already known.

The 1.5 % limit of (p´) is rather high, and difficult to achieve in practice especially in thick slabs; therefore the analysis was made for the whole range of (p´) to show the effect of such high amounts of reinforcement, but the values adopted for practical use should be restricted to the range 0.25 -1.0 %.

4.3.2 Effect of reinforcement

Analysis results are demonstrated in fig. 4.3.1, and 4.3.2, and in Appendix A; which show the possibility of reducing, or even eliminate warping deflection in floor slabs by adding upper steel. The amount of upper steel required to obtain a certain reduction in warping depends, among other things, on the amount of lower steel. The use of large amount of lower steel (p) increases warping, especially in correlation with high values of both (γ), and (T_{egr}) The time, at which the desired effect is expected, is also a factor in the process.

4.4 Analysis of loaded reinforced slabs

4.4.1 Assumptions and parameters

The analysis is performed on a 8.0 x 8.0 m slab with external, and initial shrinkage loads. The six cases of external loading involve applying two different values of distributed loads (q), 15.0, and 30.0 kN/m^2 to six different influence areas. The Influence areas are:

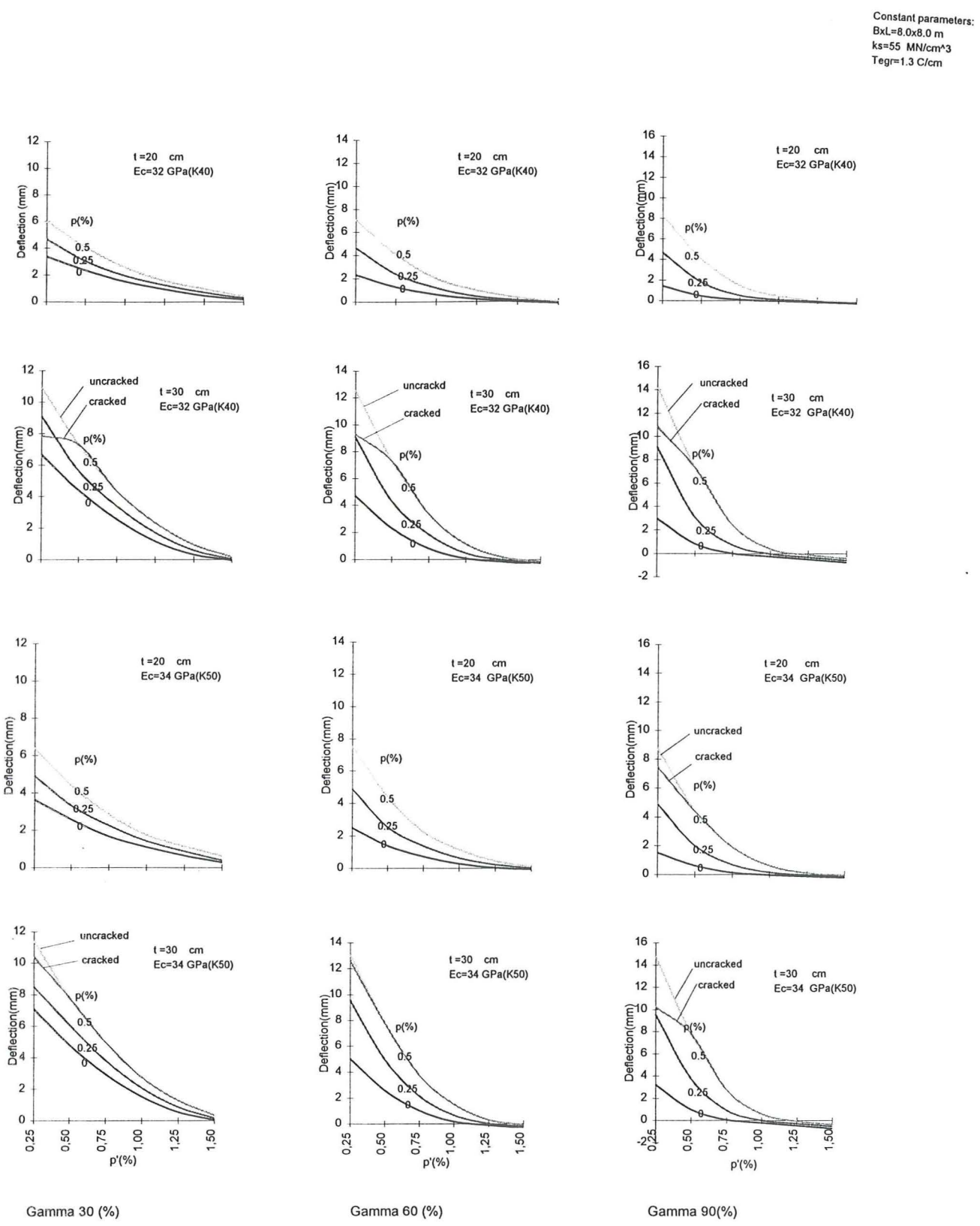

Fig. 4.3.1--Warping deflection for various values of (p), (p'), (t), (Ec) and gamma.

two edge strips, two central strips, and two central squars. Concentrated loads are considerd irrelevant to this study. Initial loading corresponds to an equivalent thermal gradient Tegr equal to 1.3 C/cm.

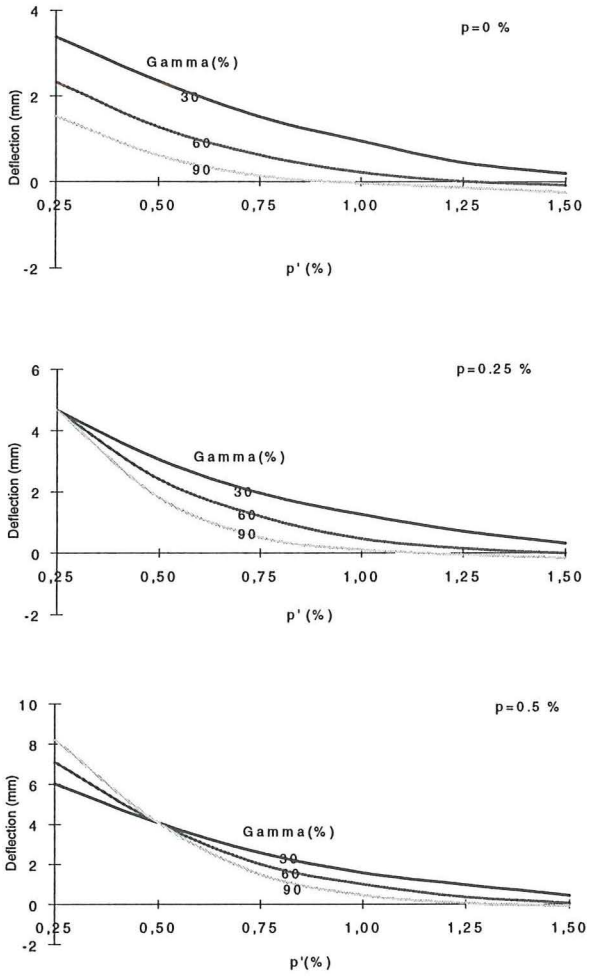

Fig. 4.3.2 — Warping deflection for various values of (p), (p´), and (γ).

The time factor (γ) is set to 30, and 60 %. The value of the other basic parameters are t = 20 cm, E_c = 32.0 GPa, f_{ct} = 1.95 MPa, and k_s = 55.0 MN/m^3.

The effect on warping of each case of loading is investigated for all reinforcement combinations The results are presented in figs. 4.4.1, and 4.4.2, and in other tables, and diagrams in the Appendix B.

4.4.2 Effect of load

It is obvious from the analysis results that the effect of loading on warping deflection is minimal. In case of edge loading, only the loaded edge is affected, while the deflection of the unloaded side remains unchanged for both values of (q); and in case of central loading (square loading at the center), deflection of the corner is slightly increased.

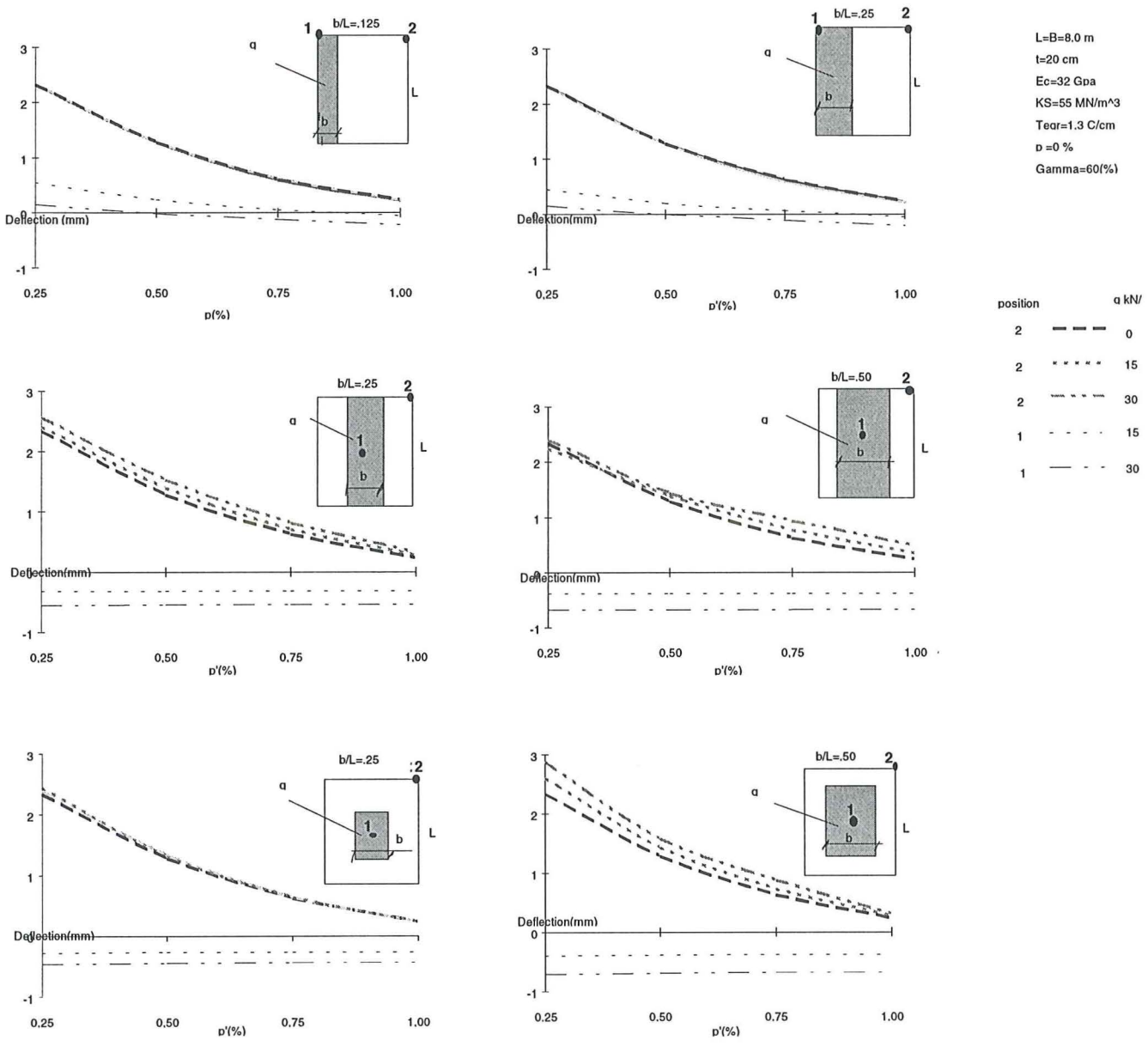

Fig. 4.4.1 – Result of analysis of six load cases for various combinations of reinforcement, with (γ) equal to 30%.

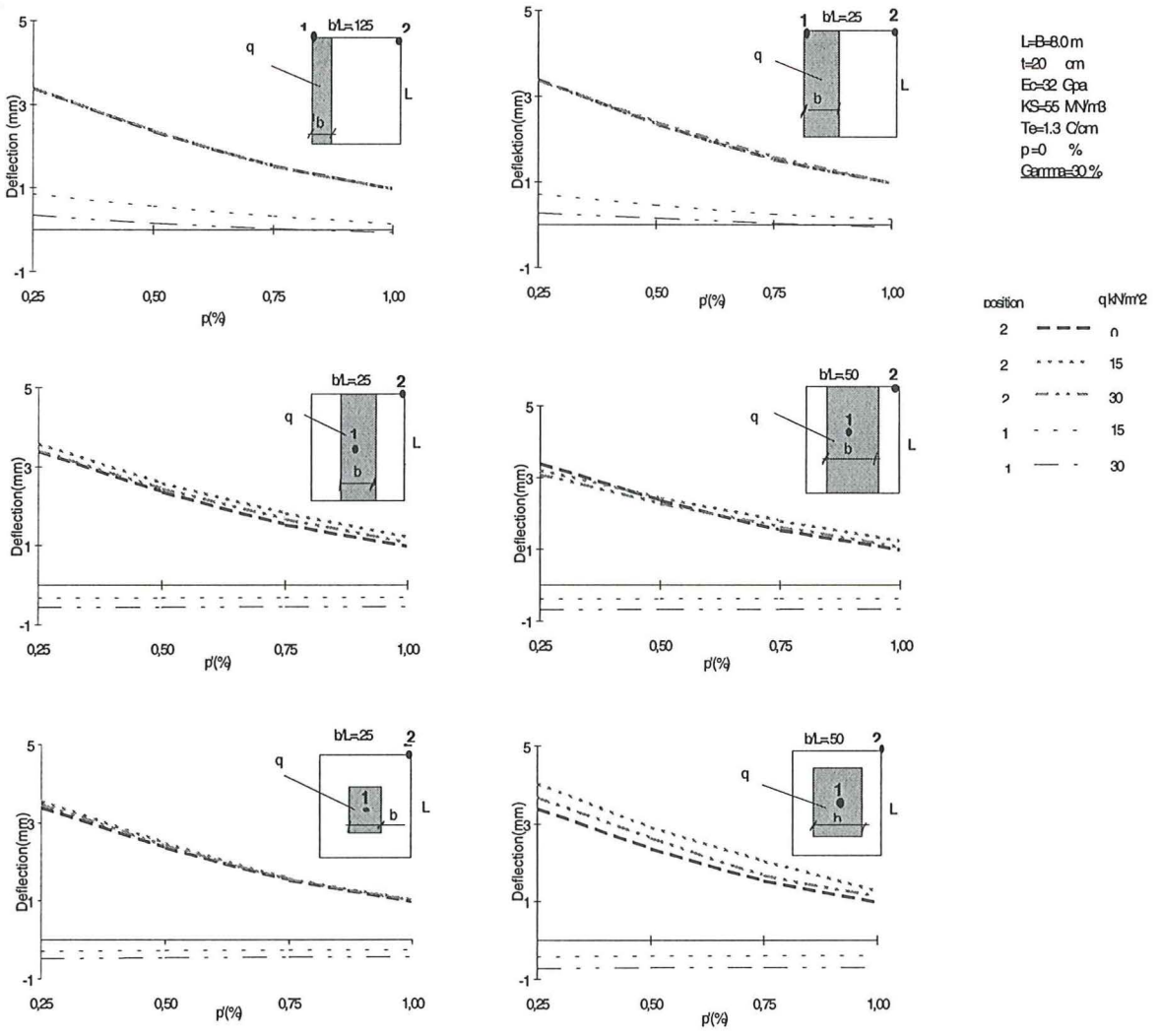

Fig. 4.4.2 — Results of analysis of six load cases for various combinations of reinforcement, with (γ) equal to 60%.

.

The obvious difference between the results of the unloaded-, and the loaded cases is noticed in the shape and extent of the contact area, and in the shape of the moment diagram. The moment is generally reduced, in some cases greatly reduced, as the warped portions of the slab are forced down into the ground.

5

Design Principles for Industrial Floors

5.1 Preliminary remarks

In chapter 4, the role of reinforcement in controlling warping in concrete slabs on grade is highlighted. The effect of many other factors on the magnitude of warping is also covered.

In this chapter, some design principles and requirements are reviewed briefly. Most of the theory background for these measures is widely known except for few points where the reader is referred to a reference. In addition to the use of steel reinforcement against warping, the problem of controlling the undesirable effects of shrinkage in floors will be addressed from a different angle by treating the source of the problem, that is, the shrinkage itself. Magnitude and distribution of shrinkage in concrete floors are influenced by several factors many of which can be manipulated to produce concrete floors with less shrinkage (both symmetrical and differential). The factors influencing shrinkage are

1. Composition and fineness of cement.
2. Cement and water content.
3. Type and gradation of aggregates.
4. Admixtures.
5. Reinforcement.
6. Friction between the floor slab, and subgrade.
7. Absorptiveness of the subgrade.

The magnitude of warping in the concrete floor is also influenced, as shown in chapter 4, by additional factors like modulus of elasticity of concrete, modulus of subgrade reaction, equivalent temperature gradient, slab thickness, and slab length (up to the critical length).

The detailed effect on concrete shrinkage, of each one of the above seven factors and many others, is explained by a vast number of books and magazines which deal with concrete. This chapter will, therefore, be limited to briefly review principles designed to benefit from the above mentioned factors to produce concrete floors with less curling and cracking.

Since the magnitude and distribution of shrinkage in concrete floors change with time, and since the amount of reinforcement required to reduce curling is much more than is normally specified, it is obvious that addition of reinforcement can not efficiently deal with the problem. Therefore, the solution to curling and cracking in concrete floors lay in a combination of supplementary reinforcement, and some measure to limit shrinkage of concrete.

5.2 Reinforcement

The first measure against shrinkage effects in floor slabs is by reinforcing the top half of the slab. The effectiveness of this action was clearly demonstrated in chapter 4, and in other studies. See for instance fig. 5.2.1 from Abdul-Wahab,[3] which shows how different amount of reinforcement in the top and bottom halves of the test beams influence curling.

As has been explained before in this study, the reinforcement in the top half reduces curling by simply restraining volume changes due to shrinkage. It has long been known that placing reinforcement in the top half has this favorable effect. Many specifications recommended that shrinkage reinforcement should be placed so. But what this study has revealed, as well as the study of Abdul-Wahab,[3] is the need for higher percentages of steel reinforcement for the sole use of curbing slab curling.

Slab curling is confined to the area adjacent to the curled joint. In most cases, the overhanging slab portion is not more than 1.5 m wide. Therefore, reinforcement should be increased at the slab edges. One percent top reinforcement could be justified in the direction perpendicular to and for 3.0 m from the slab edge, as suggested by Ytterberg[5] (Part III)

5.3 Concrete mix design

The design of the concrete mix for the floor slab may be the most efficient way of controlling shrinkage in concrete; therefore, special attention should be given to it by the designers. The aim is to produce a concrete mix with very high workability; yet with minimum amount of shrinkage without the use of admixtures.

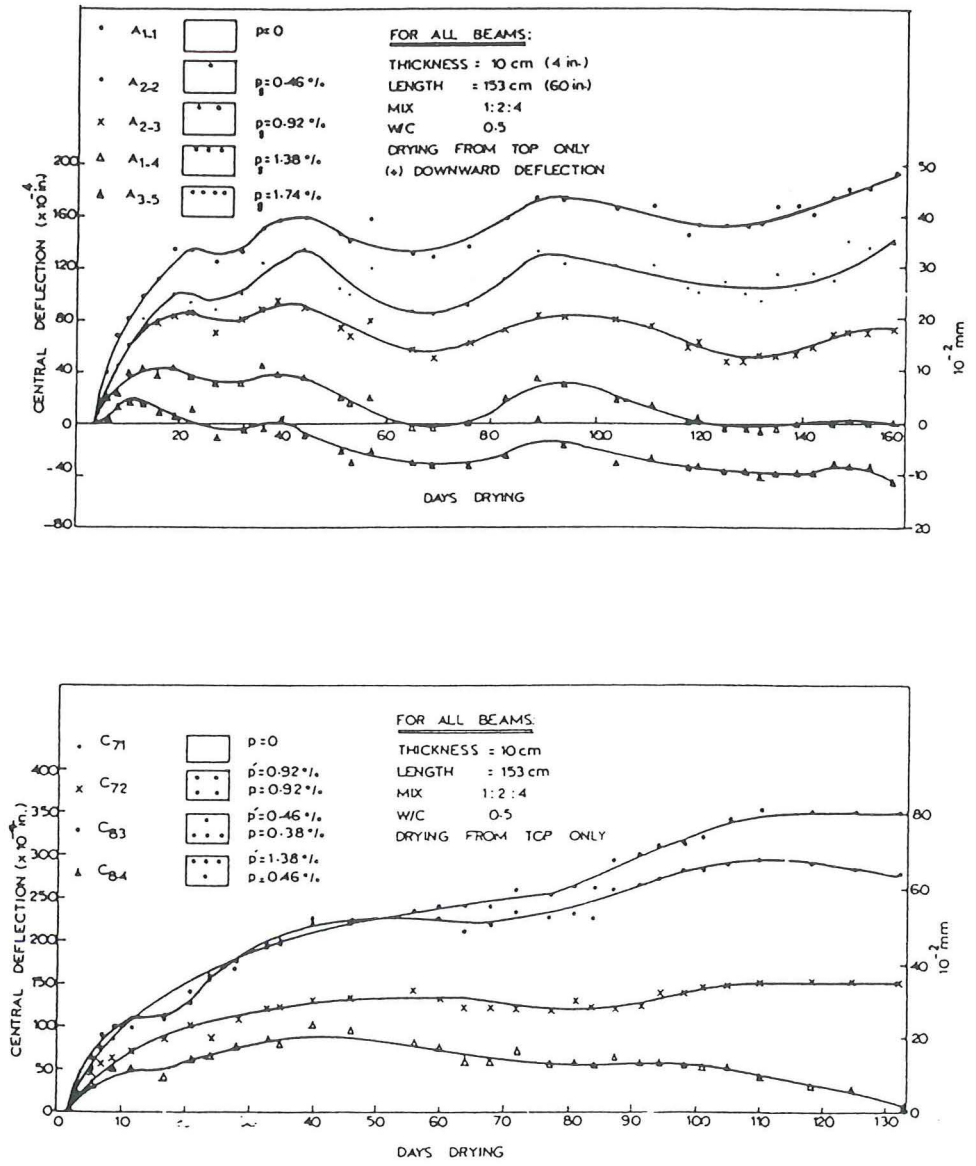

Fig. 5.1.1 — The effect of different types of reinforcement on time-deflection curve for two groups of beams. From Abdul-Wahab[3]

These, seemingly, contradicting requirements can be fulfilled by the following

1. A more uniform than normal aggregate distribution, with more middle aggregate sizes.
2. Aggregates which have a high percentage of large-size stones. The combination of this demand and (1) above would make the mix very stony but very workable one, and would minimize the cement paste (the main source of shrinkage in concrete).
3. Natural sand rather than sand produced from stone crushing, because natural sand is smoother; hence enhances workability, and reduces water and cement requirements.

4. Type II-cement or any other type of cement with low shrinkage characteristics, and which yield low heat of hydration. Coarser ground cements are also advisable.
5. Aggregates of low absorptiveness, and low drying shrinkage
6. Minimize or eliminate the use of admixtures as they may cause considerable increase in shrinkage.
7. Keep the temperature of placed concrete appropriately low to reduce the quantity of water lost by evaporation.

These measures are designed to gain the following advantages

1. Far more workable mix.
2. Less cement and water requirement.
3. Bleeding and segregation are minimized.
4. Less shrinkage, creep, and curl.

5.4 Use of shrinkage compensating cement

The use of concrete made with expansive cement (also called shrinkage compensating cement, or cement Type K) may result in floor slabs with an ultimate concrete shrinkage equal to zero, and reduce the joints significantly.

The difference between this type of cement and common Portland cement is that shrinkage compensating cement expands in the first few days after casting, and then when the concrete in exposed to drying conditions, it will shrink.

As concrete made with expansive cement begins to set, bond with reinforcement starts to develop, and at the same time, the gradual expansion in concrete continues. This expansion sets the reinforcement in tension and the concrete in compression; hence, lightly prestressing the slab.

Later, when the concrete is exposed to drying conditions, it starts to shrink, but unlike the common Portland cement concrete, the shrinkage in expansive concrete will only relieve the prestressing built in the slab during expansion process.

5.5 Use of steel fiber reinforced concrete

Another approach to solve the problems associated with concrete floors especially industrial floors is by the use of steel fiber reinforced concrete (SFRC) with or without other types of reinforcement. The uniform distribution of fibers in the concrete is effective in controlling shrinkage and reducing the need for closer joints.

5.6 Post-tensioning

Post-tensioning has been used to minimize possible transverse cracking, especially in long strip placements. Post-tensioning allows relatively thinner slab sections to be used, and increases slabs ability to carry heavier loads.

5.7 Location of joints

It is sometimes possible to correlate the location of joints in industrial floor slabs with the location of storage racks. If so is the case, it is beneficial to place the storage racks along the joints leaving a clear aisle in the middle for truck traffic. Aisles are kept without transverse construction and contraction joints to avoid slab curling immediately adjacent to those joints with the ultimate breakdown of the curled portions under the repeated traffic loads.

Larger slabs are more advisable as there is no risk of increasing the magnitude of curling beyond that produced at slab length equal to the critical length. Adopting larger slabs is designed to minimize the number of curled joints. The increase in magnitude of shrinkage in the larger slabs must be counterbalanced by placing shrinkage reinforcement near the top surface of the slab. The amount of such reinforcement is calculated by the subgrade drag formula, which is

$$A_s = 0.5\ F\ L\ w\ /\ f_s \qquad (5.7.1)$$

where

A_s	steel reinforcement cross-sectional area
F	coefficient of subgrade friction
L	slab length (or width) between joints
w	Weight of slab per unit area
f_s	allowable stress of reinforcement

Reinforcement according to this formula will minimize crack width, but will increase cracking, and it will only contribute to the load carrying capacity of the slab in locations of negative bending moment.

5.8 Eliminating restraint

As the tendency of slab construction is getting toward constructing larger slabs with less joints, noticeable movement of slabs must be expected due to shrinkage, or to post-tensioning (if the slab is post-tensioned). Differential movements between adjacent slabs may also occur due to the different conditions of each slab. Therefore, proper attention should be paid to eliminating restraint of volume changes in the slab.

Restraints which should be investigated at the design stage are the restraint provided by dowels, and by features penetrating the floor slab like roof columns and machine foundations.

Dowels are essential to transfer shear from one slab to another, but the type of dowels normally used in such cases (round bars) cause serious cracking problems. Horizontal movement of the slab is restrained by misaligned dowels laid parallel to the movement direction, or by the dowels of the joints parallel to the movement. Another case of restraint is caused by dowels between a new and an older slab. See fig. 5.8.1

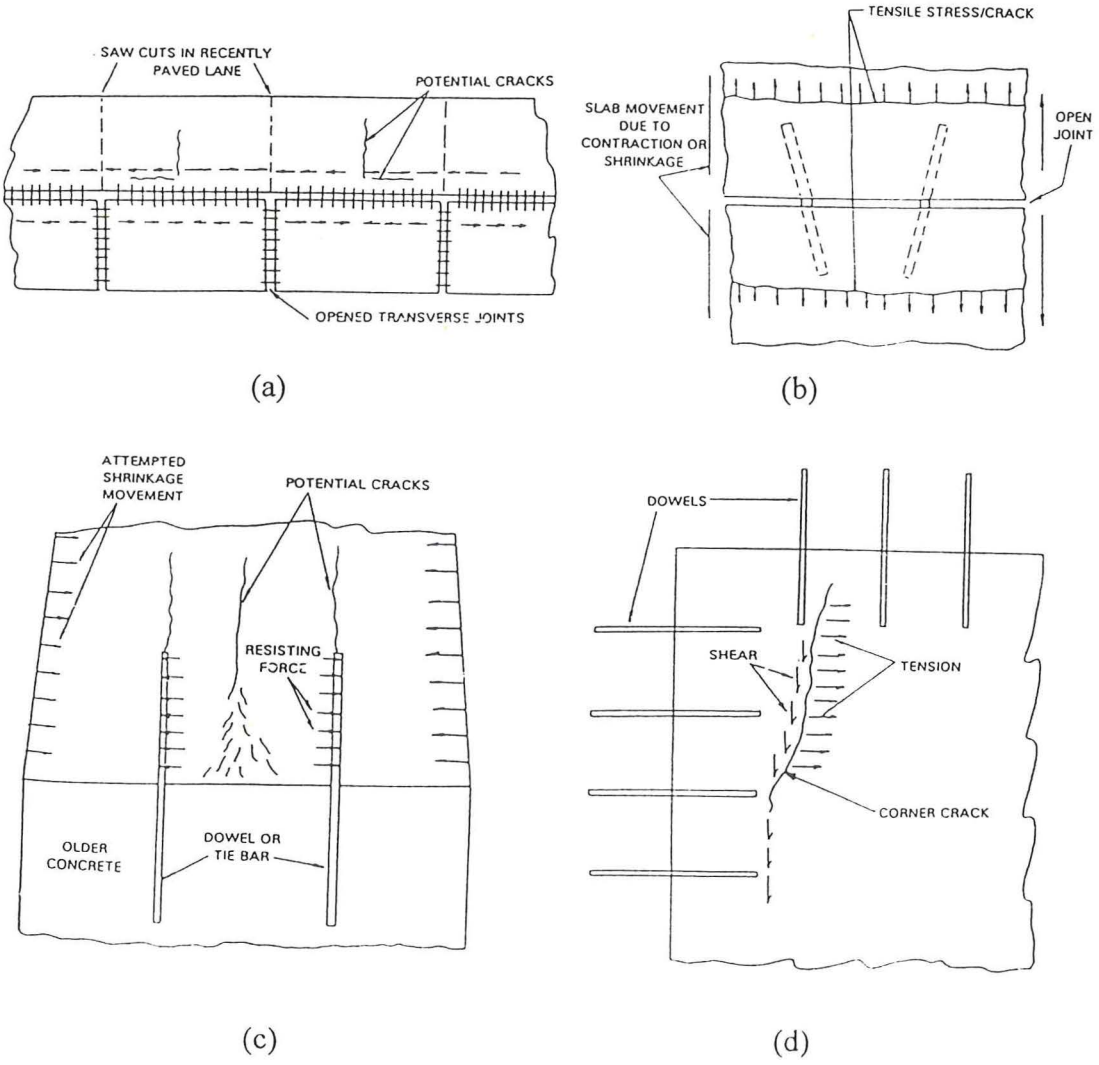

a — Dowel restraint between old and new slab.
b — Misaligned dowels have to bend to allow slab movement.
c — Detail of dowel restraint between old and new slab.
d — Cracking of slab corner.

Fig. 5.8.1 — Cracking due to dowel restraint. From Schrader[17]

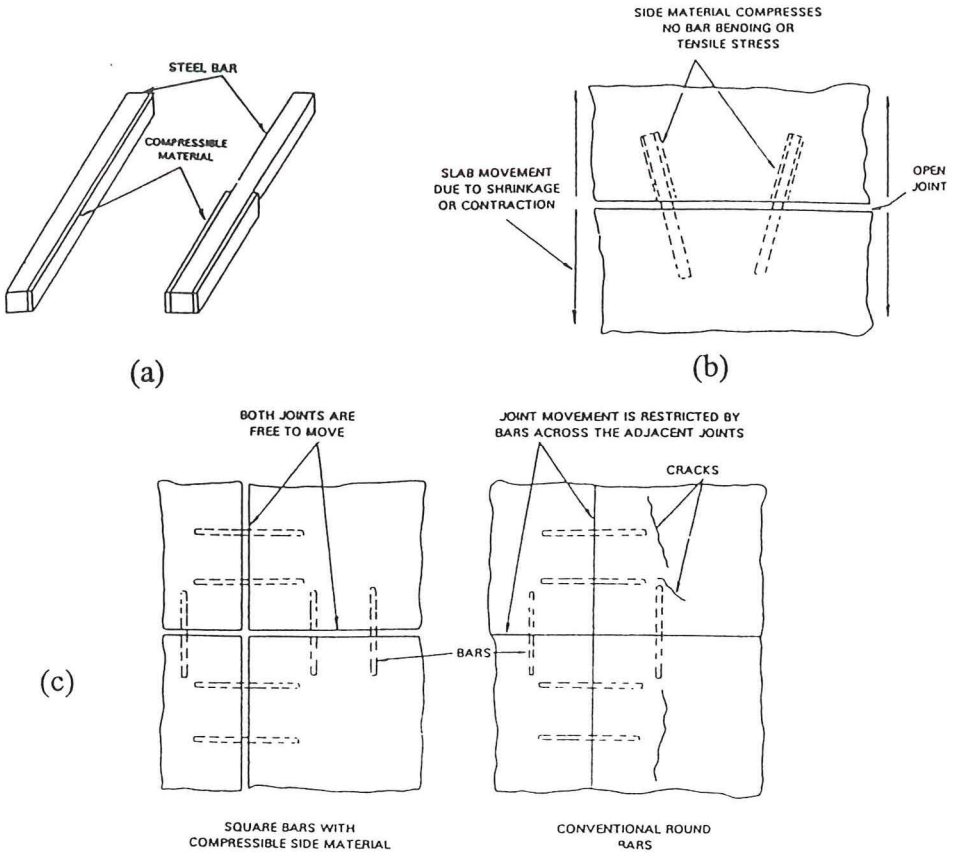

Fig. 5.8.2 — The solution to dowel restraint by square dowels with cushioning sides as in (a) which do not restrain slab movement when the dowels are misaligned (b), or at the corners (c). From Schrader[17]

The solution to this problem is by using lightly greased, square dowels with cushioning side pads, as shown in fig. 5.8.2, which only allow the horizontal differential movement of the slab (no vertical differential movement).

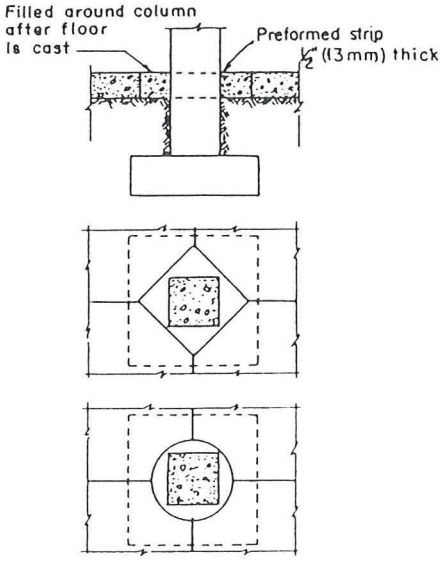

Fig. 5.8.3 — Shape of joint around features penetrating the floor slab. From ACI Committee 302.[18]

5.9 Upgrading the soil bearing capacity

The bearing capacity of the subgrade, expressed as modulus of subgrade reaction k_s , can be increased by using treated or untreated subbase. The increase in k_s value produces higher warping stresses which increases cracking in the slab. However, the advantage of increasing the modulus of subgrade reaction is to reduce the need for flexural reinforcement near the bottom of the slab, and to reduce the slab thickness required to carry a certain loading.

It was shown in chapter 4, that magnitude of curling increases with the increase in lower reinforcement, and with the increase in thickness (if the equivalent temperature gradient was assumed to be variable, and ΔT was kept constant); Therefore, upgrading the modulus of subgrade reaction results indirectly in reducing slab curling.

The k_s value can be increased by several methods, for instance, according to Ritter and Paquette (pp. 688),[19] for a subgrade with a k_s value of 100 lb/in^3 (27.7 MN/m^3), a 4-inch (10 cm) cement treated base course should increase k_s value to at least 300 lb/in^3 (83.0 MN/m^3).

5.10 Improving the subgrade conditions

Higher moisture content in the subgrade results in reduction in the amount of water leaving the slab bottom, or even increase the moisture content near the bottom; hence, increasing the equivalent temperature gradient, and consequently increases curling. For the same reason, a permeable dry subgrade will reduce curling.

To offset this effect, it is recommended that an impermeable vapor barrier is laid under the slab and covered with crushed stones and finished with a thin layer of sand. This arrangement will prevent ground water from reaching the slab, and in the same time, will make it easier for the water to leave the bottom of the slab. The sand layer may also reduce the friction between the slab and the subgrade.

5.11 Reducing modulus of elasticity of concrete

According to Sec. 4.2.5, the magnitude of curling in a concrete slab is proportional to the modulus of elasticity of concrete. Leaner concrete give rise to less slab curling and less curling stress which means less cracking.

The modulus of elasticity of concrete E_c varies with strength. The strength of concrete is controlled by proportioning the components of the concrete mix. Water-cement ratio, and the amount of cement in the mix greatly influence the strength.

The use of less cement in the mix (as recommended for a different reason by Sec. 5.3) result in less curling, because the reduction in cement will give two useful results: (1) less shrinkage as a direct result of cement reduction itself, and (2) Concrete with less strength, i.e. less E_c which will yield less curling.

6

Conclusions

Curling or warping is a common event in all types of slabs on grade. Slab edges curl upward and loose contact with the subgrade, and slab center sinks slightly into the ground. In industrial floors, the reason for curling is the presence of a negative shrinkage gradient across the depth of the slab caused by differential dryness. Slabs dry much faster from its top than from its bottom; thereby, causing different shrinkage across the depth.

Warping (as curling is also called) causes many problems. It degrades the performance of industrial floors as a platform for transport equipment. In addition, warped floors are partially supported, so heavy truck loads passing over the overhanging slab may cause it to breakdown.

This phenomenon has been known for a relatively long time; Nevertheless, the only action against it has been the use of closer spacing between the joints, and the introduction of supplementary steel to control shrinkage cracking. Furthermore, the current methods of design of slabs-on-grade assume that slabs are in full contact with the ground.

The first objective of this work is to prepare a FEM-model to analyze the response of slabs-on-grade to various parameters thought to have influence on warping. These factors are: material properties, slab dimensions, strain gradient, and imposed loads. Material properties include properties of concrete, steel reinforcement, and subgrade. The FEM-formulation is implemented as supplementary functions and batch files in CALFEM which includes the basic functions of a FEM-program.

The FEM analysis confirms the role of the upper steel reinforcement in reducing or even eliminating warping in slabs-on-grade. However, the amount of upper steel required to achieve this goal is found to be much higher than the amount of shrinkage steel normally used in reality. In some cases this amount is too high to be implemented under the current rules of concrete design. The lower steel, specified for flexure, increases warping in floor slabs, and requires more warping steel to be placed at the upper half of the slab section. It is therefore important to supplement warping steel with other measures.

These additional measures should be designed to produce concrete with limited shrinkage, and to improve construction methods of floor slabs to minimize the shrinkage gradient.

The influence of thickness on warping can not be established with certainty. The relation between the equivalent thermal gradient used to describe the shrinkage gradient, and the change in thickness is not clear. Two alternatives can be assumed when slab thickness is changed: (1) The equivalent thermal gradient remains constant, and (2) The shrinkage strain at the top fiber remains constant. In this study, the first alternative is adopted everywhere except for thickness control, where both alternatives are checked.

Further studies are needed to highlight this matter, and to find out the values of shrinkage and equivalent temperature gradient encountered in reality. The general verification of the results of this study experimentally is also needed.

Appendix

APPENDIX A

Analysis results of unloaded reinforced floor slabs.

Table A.1---Analysis of reinforced floor slab.

t=20 cm																							
		Ec = 32 Gpa , fct = 1,95 Mpa (K 40)												Ec = 34 Gpa , fct = 2,25 Mpa (K 50)									
Reinf.		crack moment		Mmin(kNm/m)			Mmax(kNm/m)			Def(mm)				crack moment		Mmin(kNm/m)			Mmax(kNm/m)			Def(kNm/m)	
p	p'	Mcr(-)	Mcr(+)	gamma			gamma			gamma				Mcr(-)	Mcr(+)	gamma			gamma			gamma	
(%)	(%)	(kNm/m)	(kNm/m)	0,30	0,60	0,90	0,30	0,60	0,90	0,30	0,60	0,90		(kNm/m)	(kNm/m)	0,30	0,60	0,90	0,30	0,60	0,90	0,30	0,60	0,90
	0,25	-10,58	10,23	-6,32	-3,55	-2,69	0,16	0,36	0,21	3,38	2,33	1,43		-12,19	11,82	-6,32	-4,15	-2,70	0,09	0,39	0,21	3,62	2,51	1,52
	0,50	-10,75	10,07	-3,55	-2,69	-0,59	0,36	0,21	0,05	2,35	1,28	0,47		-12,38	11,64	-4,15	-2,70	-1,34	0,39	0,21	0,12	2,58	1,40	0,61
0,00	0,75	-10,92	9,93	-2,69	-1,33	-0,33	0,21	0,12	0,33	1,52	0,62	0,10		-12,56	11,48	-2,70	-1,87	-0,57	0,21	0,31	0,12	1,67	0,72	0,14
	1,00	-11,09	9,79	-2,69	-0,59	-0,02	0,21	0,05	0,26	0,95	0,22	-0,05		-12,75	11,33	-2,70	-0,59	-0,02	0,21	0,05	0,26	1,13	0,28	-0,03
	1,25	-11,26	9,66	-0,59	-0,02	-0,02	0,05	0,26	0,26	0,45	0,01	-0,15		-12,93	11,20	-1,34	-0,02	-0,02	0,12	0,26	0,26	0,64	0,04	-0,14
	1,50	-11,42	9,55	-0,59	-0,02	-0,02	0,05	0,26	0,26	0,20	-0,08	-0,25		-13,11	11,07	-0,59	-0,02	-0,02	0,05	0,26	0,26	0,29	-0,05	-0,24
	0,25	-10,40	10,40	-6,32	-6,32	-6,32	0,16	0,16	0,16	4,65	4,65	4,65		-12,00	12,00	-6,32	-6,32	-6,32	0,09	0,09	0,09	4,90	4,90	4,90
	0,50	-10,57	10,24	-6,32	-3,55	-2,69	0,16	0,36	0,21	3,04	2,33	1,62		-12,18	11,82	-6,32	-4,15	-2,70	0,09	0,39	0,21	3,32	2,54	1,74
0,25	0,75	-10,73	10,09	-2,69	-2,69	-0,59	0,21	0,21	0,05	1,87	1,19	0,50		-12,36	11,66	-3,57	-3,05	-1,51	0,35	0,26	0,47	2,26	1,38	0,68
	1,00	-10,90	9,95	-2,69	-0,59	-0,22	0,21	0,05	0,35	1,26	0,46	0,10		-12,54	11,50	-2,70	-1,51	-0,57	0,21	0,47	0,12	1,43	0,64	0,14
	1,25	-11,06	9,81	-1,50	-0,56	-0,02	0,48	0,11	0,26	0,70	0,14	-0,06		-12,72	11,36	-2,70	-0,59	-0,02	0,21	0,05	0,26	0,87	0,22	-0,04
	1,50	-11,22	9,69	-0,59	-0,02	-0,02	0,05	0,26	0,26	0,31	-0,01	-0,17		-12,89	11,23	-0,59	-0,02	-0,02	0,05	0,26	0,26	0,40	0,01	-0,15
	0,25	-10,24	10,57	-7,76	-8,76	-9,48	0,02	0,02	-0,04	6,02	7,09	8,21		-11,82	12,18	-8,79	-9,50	-12,62	0,02	-0,05	-0,11	6,40	7,51	8,78
	0,50	-10,40	10,40	-6,93	-6,93	-6,93	0,16	0,16	0,16	4,07	4,07	4,07		-12,00	12,00	-6,94	-6,94	-6,94	0,07	0,07	0,07	4,40	4,40	4,40
0,50	0,75	-10,56	10,24	-4,14	-2,69	-2,69	0,41	0,21	0,21	2,57	1,87	1,49		-12,17	11,83	-4,87	-3,57	-2,70	0,33	0,35	0,21	2,84	2,25	1,63
	1,00	-10,72	10,10	-2,69	-2,69	-0,59	0,21	0,21	0,05	1,57	0,99	0,45		-12,35	11,67	-2,70	-2,70	-1,34	0,21	0,21	0,12	1,75	1,15	0,61
	1,25	-10,88	9,96	-2,69	-0,59	-0,02	0,21	0,05	0,26	0,96	0,36	0,04		-12,52	11,52	-2,70	-0,59	-0,33	0,21	0,05	0,34	1,15	0,44	0,10
	1,50	-11,03	9,84	-0,59	-0,02	-0,02	0,05	0,26	0,26	0,43	0,05	-0,08		-12,69	11,38	-1,34	-0,65	-0,02	0,12	0,23	0,26	0,63	0,12	-0,06
t=30 cm																							
	0,25	-23,88	22,94	-18,53	-14,02	-10,91	0,00	-0,14	-0,15	6,68	4,71	2,96		-27,52	26,50	-20,16	-14,24	-12,63	-0,19	-0,14	-0,13	7,10	5,05	3,23
	0,50	-24,36	22,51	-14,02	-9,14	-3,82	0,00	0,19	0,34	4,39	2,32	0,83		-28,04	26,04	-14,24	-9,85	-5,11	-0,14	0,07	-0,07	4,83	2,62	1,00
0,00	0,75	-24,83	22,13	-9,69	-3,82	0,01	0,07	0,34	0,55	2,55	0,82	0,02		-28,55	25,61	-11,01	-5,11	-0,15	-0,16	-0,07	0,51	2,96	1,04	0,08
	1,00	-25,30	21,77	-4,37	-0,15	0,01	0,00	0,50	0,55	1,16	0,09	-0,25		-29,05	25,22	-6,06	-1,06	0,02	0,10	0,28	0,56	1,54	0,18	-0,21
	1,25	-25,76	21,44	-1,08	0,01	-0,23	0,00	0,55	1,29	0,32	-0,16	-0,51		-29,55	24,85	-2,18	0,02	0,02	0,21	0,56	0,56	0,55	-0,11	-0,47
	1,50	-26,22	21,13	0,01	0,01	-2,80	0,55	0,55	7,57	-0,02	-0,39	-0,77		-30,05	24,51	0,02	0,02	-3,10	0,56	0,56	5,58	0,04	-0,33	-0,72
	0,25	-23,40	23,40	-23,23	-23,23	-23,23	0,00	-0,19	-0,19	9,10	9,10	9,10		-27,00	27,00	-23,45	-23,45	-23,45	-0,18	-0,18	-0,18	9,56	9,56	9,56
	0,50	-23,86	22,96	-17,91	-12,49	-10,91	0,00	-0,12	-0,15	5,63	4,29	3,07		-27,50	26,52	-18,15	-14,24	-12,63	-0,19	-0,14	-0,13	6,11	4,71	3,43
0,25	0,75	-24,31	22,55	-12,49	-6,74	-2,69	0,00	0,14	0,24	3,37	1,84	0,73		-27,99	26,08	-12,63	-9,28	-5,11	-0,13	0,18	-0,07	3,85	2,17	0,93
	1,00	-24,76	22,18	-6,00	-2,17	0,01	0,10	0,21	0,55	1,71	0,49	-0,02		-28,48	25,67	-6,78	-2,72	0,02	0,13	0,24	0,56	2,09	0,68	0,02
	1,25	-25,21	21,84	-2,69	0,01	0,01	0,24	0,55	0,55	0,60	-0,03	-0,31		-28,96	25,29	-4,29	0,02	0,02	0,25	0,56	0,56	0,87	0,03	-0,26
	1,50	-25,65	21,51	0,01	0,01	-0,60	0,55	0,55	1,76	0,05	-0,27	-0,58		-29,44	24,93	-0,80	0,02	-0,23	0,50	0,56	1,31	0,17	-0,21	-0,53
	0,25	-22,96	23,86	-26,88	-26,88	-26,88	0,00	-0,08	-0,08	10,92	12,58	14,23		-26,52	27,50	-27,13	-27,13	-32,74	-0,07	-0,07	0,10	11,41	13,07	14,79
	0,50	-23,40	23,40	-19,97	-19,97	-19,97	0,00	-0,19	-0,19	7,29	7,29	7,29		-27,00	27,00	-23,45	-23,45	-23,45	-0,18	-0,18	-0,18	7,83	7,83	7,83
0,50	0,75	-23,84	22,98	-14,02	-12,49	-9,14	0,00	-0,12	0,19	4,34	3,33	2,42		-27,47	26,54	-14,24	-12,63	-10,28	-0,14	-0,13	-0,10	4,85	3,79	2,80
	1,00	-24,27	22,59	-9,14	-4,37	-1,08	0,19	-0,21	-0,05	2,32	1,16	0,40		-27,95	26,12	-10,28	-6,06	-2,72	-0,10	0,10	0,24	2,77	1,53	0,62
	1,25	-24,70	22,23	-5,07	-0,80	0,01	0,00	0,51	0,55	0,95	0,17	-0,11		-28,41	25,72	-6,06	-1,09	0,02	0,10	-0,07	0,56	1,30	0,31	-0,06
	1,50	-25,12	21,90	-1,19	0,01	0,01	0,34	0,55	0,55	0,18	-0,14	-0,40		-28,87	25,35	-1,09	0,02	0,02	-0,07	0,56	0,56	0,35	-0,08	-0,35

TableA.2---Analysis of cracked reinforced section.

Cracked section				
t	gam.	K	Ie/Ig	Def.
cm	%			mm
20	90	50	0,85	7,45
30	30	50	0,95	10,39
30	60	40	0,70	9,31
30	60	50	0,95	12,63
30	90	40	0,70	10,85
30	90	50	0,62	10,24
30	30	40	0,70	7,87

Moment is larger than cracking moment; hence, moment of inertia is reduced for a second analysis.

Table A.3 --- Section geometry for various t values.

t (mm)	Section Dimension	Bar Size (mm) 8	12	16	20	25	32
150	dx	126	124	122	120	117,5	114
	dy	118	112	106	100	92,5	82
	dx'	24	26	28	30	32,5	36
	dy'	32	38	44	50	57,5	68
200	dx	176	174	172	170	167,5	164
	dy	168	162	156	150	142,5	132
	dx'	24	26	28	30	32,5	36
	dy'	32	38	44	50	57,5	68
250	dx	226	224	222	220	217,5	214
	dy	218	212	206	200	192,5	182
	dx'	24	26	28	30	32,5	36
	dy'	32	38	44	50	57,5	68
300	dx	276	274	272	270	267,5	264
	dy	268	262	256	250	242,5	232
	dx'	24	26	28	30	32,5	36
	dy'	32	38	44	50	57,5	68

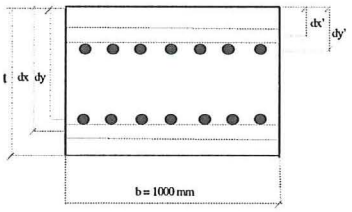

Table A.4 --- Spacing in mm, between bars for various bar sizes, reinforcement percentages, and slab thickness t = 20 cm.

		Bar size (mm)					
		8	12	16	20	25	32
t	p	Bar area (mm^2)					
cm	%	50	113	201	314	491	804
20	0,25	117	269	490	785	1266	2173
	0,5	58	135	245	393	633	1086
	0,75	39	90	163	262	422	724
	1	29	67	123	196	317	543
	1,25	23	54	98	157	253	435
	1,5	19	45	82	131	211	362
30	0,25	74	169	304	483	770	1297
	0,5	37	84	152	242	385	648
	0,75	25	56	101	161	257	432
	1	18	42	76	121	192	324
	1,25	15	34	61	97	154	259
	1,5	12	28	51	81	128	216

Table A.5 --- Strain at top fiber of slab section (*10^6).

t (cm)	Gamma (%)	T_{egr} (C/cm)		
		0,4	**0,9**	**1,3**
15	**30**	78	176	254
	60	96	216	312
	90	114	257	371
20	**30**	104	234	338
	60	128	288	416
	90	152	342	494
25	**30**	130	293	423
	60	160	360	520
	90	190	428	618
30	**30**	156	351	507
	60	192	432	624
	90	228	513	741

Table A.6 --- Steel area (mm^2/m) for various reinforcement percentages (p), and Slab thicknesses.

		Bar size (mm)				
		8	**12**	**16**	**20**	**25**
t	p	Bar area (mm^2)				
cm	%	**50**	**113**	**201**	**314**	**491**
20	**0,25**	430	420	410	400	388
	0,5	860	840	820	800	775
	0,75	1290	1260	1230	1200	1163
	1	1720	1680	1640	1600	1550
	1,25	2150	2100	2050	2000	1938
	1,5	2580	2520	2460	2400	2325
30	**0,25**	680	670	660	650	638
	0,5	1360	1340	1320	1300	1275
	0,75	2040	2010	1980	1950	1913
	1	2720	2680	2640	2600	2550
	1,25	3400	3350	3300	3250	3188
	1,5	4080	4020	3960	3900	3825

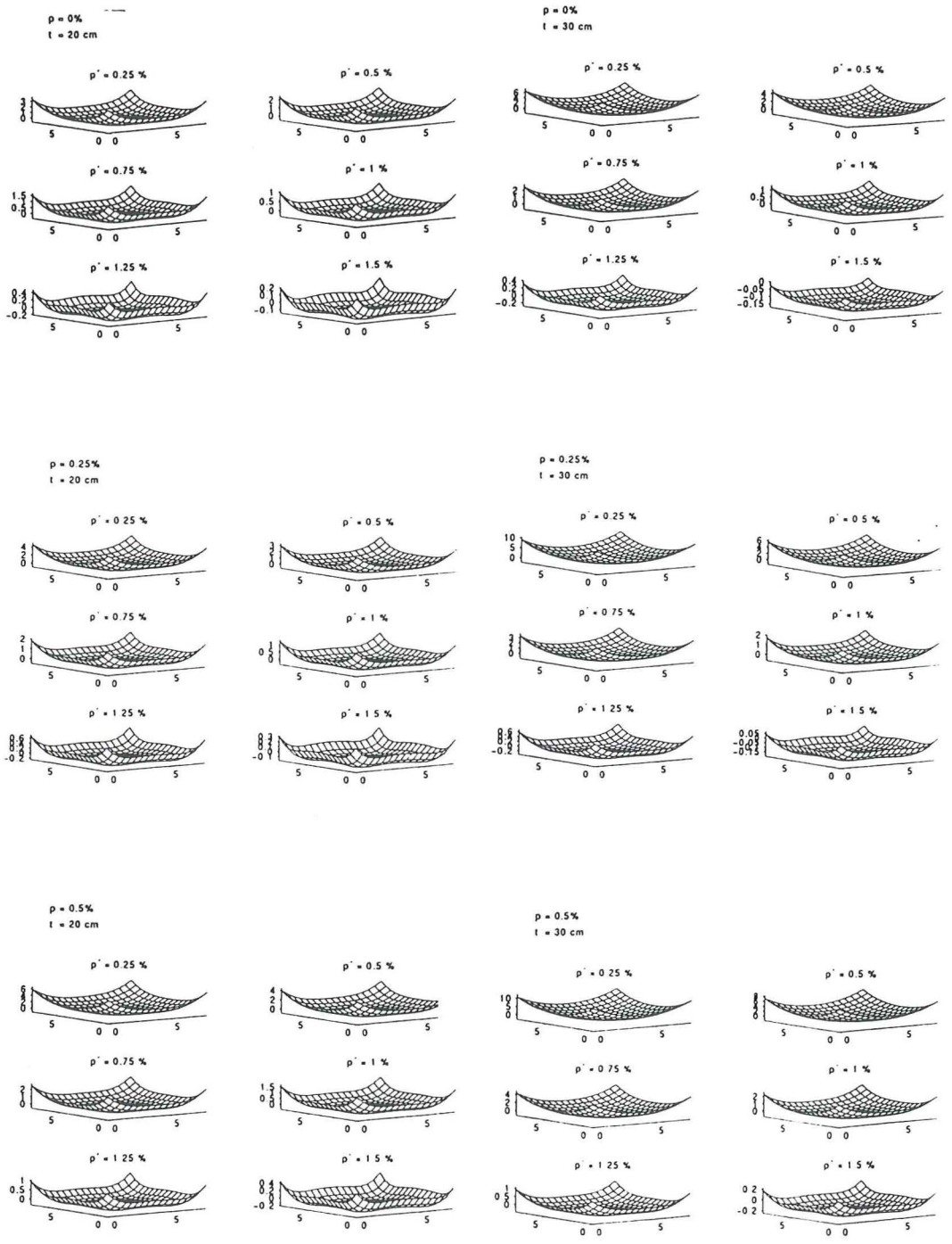

Fig. A.1— 3D representation of six sets of analyses each with different (p). Each set of figures show the change in slab warping due to change in the upper reinforcement. E_c = 32 Gpa; and γ = 30 %

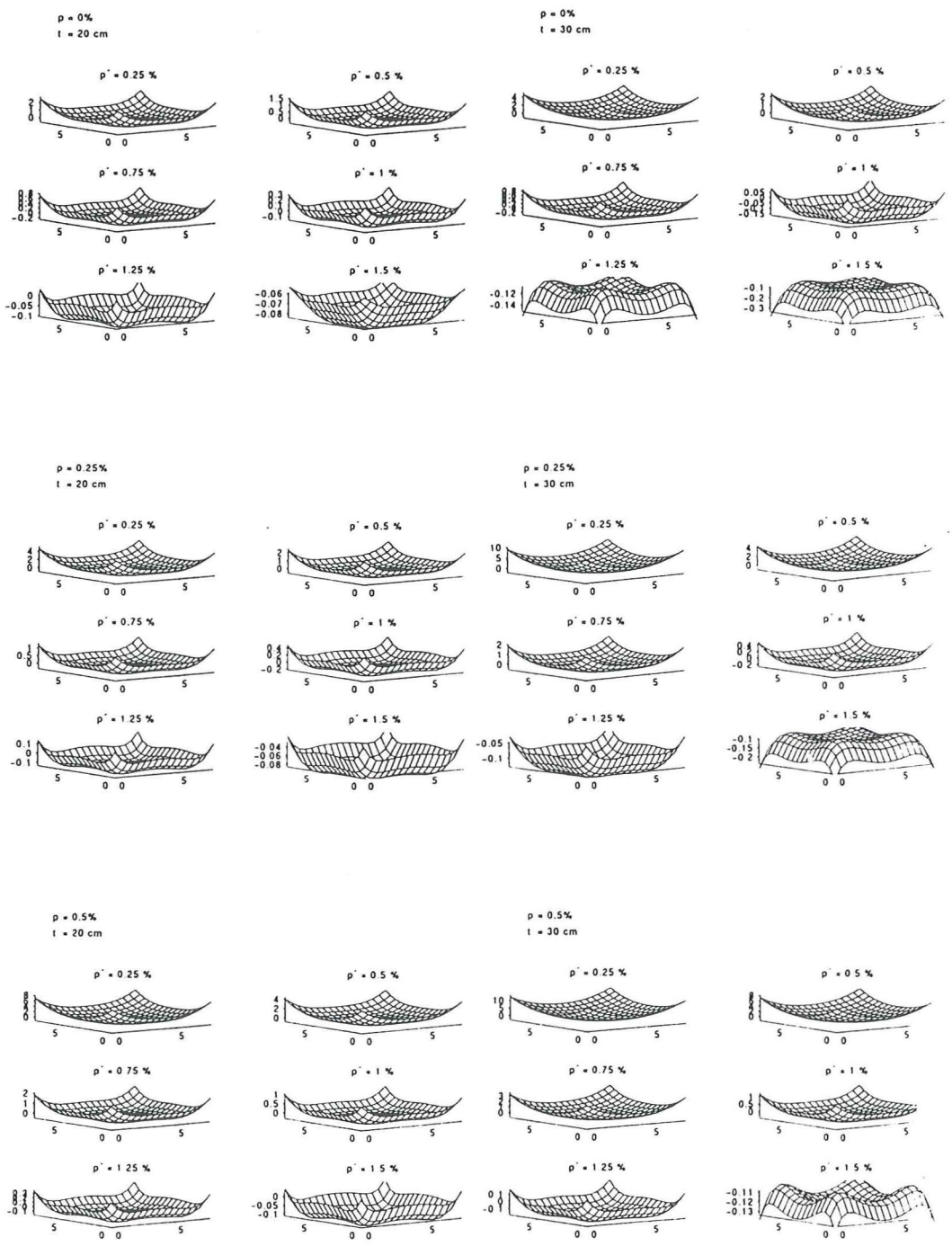

Fig. A.2 — 3D representation of six sets of analyses each with different (p). Each set of figures show the change in slab warping due to change in the upper reinforcement.
E_c = 32 Gpa γ = 60 %

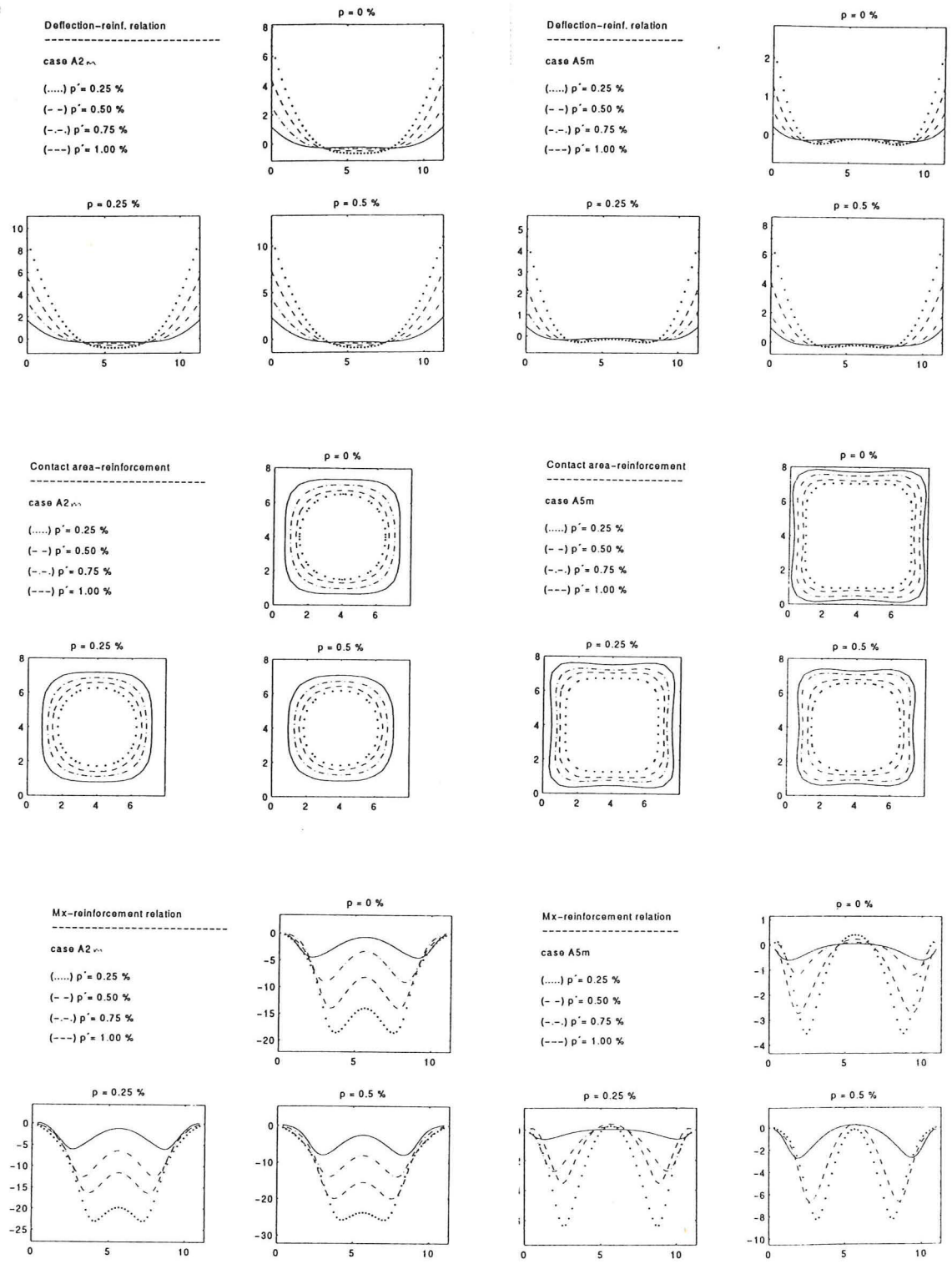

Fig. A.3 — Effect of reinforcement on: Corner deflection in mm(top), Contact area (middle), and Moment in kNm/m(bottom); $E_c = 32$ Gpa; (case A2m): $\gamma = 30$ %, t = 30 cm and (case A5m): $\gamma = 60$ %, t = 20 cm

APPENDIX B

Analysis results of loaded reinforced floor slabs.

Table B.1—Destributed load on the edge strip.

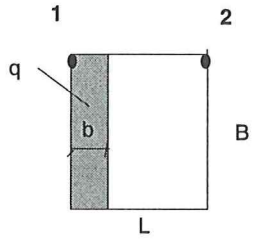

L=B=8,0m
Thickness=20cm
Ec=32,0GPa
fct=1,95MPa
ks=55,0MN/m^3
T_{φ}=1.3C/cm

b/L=0,125																					
				MMin (kNm/m)				MMax (kNm/m)				Def. (mm)									
Reinf.		crack moment		Gamma 30 %		Gamma 60 %		Gamma 30 %		Gamma 60 %		Gamma 30 %					gamma 60 %				
p	p'	Mcr(-)	Mcr(+)	q (kN/m^2)																	
(%)	(%)	(kNm/m)	(kNm/m)	15	30	15	30	15	30	15	30	15		30		unloaded	15		30		unloaded
												1	2	1	2	2	1	2	1	2	2
	0,25	-10,58	10,23	-6,06	-5,98	-3,51	-3,50	1,23	0,56	1,74	0,50	0,86	3,37	0,34	3,37	3,38	0,55	2,32	0,14	2,32	2,33
0,00	0,50	-10,75	10,07	-3,51	-3,50	-2,65	-2,62	1,74	0,50	0,30	0,79	0,55	2,35	0,15	2,35	2,35	0,24	1,28	-0,02	1,28	1,28
	0,75	-10,92	9,93	-2,65	-2,62	-0,92	-0,93	0,33	0,51	0,30	0,96	0,32	1,51	0,02	1,51	1,52	0,05	0,59	-0,12	0,59	0,62
	1,00	-11,09	9,79	-2,65	-2,62	-0,58	-0,58	0,30	0,79	0,57	1,00	0,14	0,95	-0,07	0,95	0,95	-0,06	0,22	-0,22	0,22	0,22
	0,25	-10,40	10,40	-6,10	-5,98	-6,10	-5,98	0,27	0,61	0,27	0,61	1,40	4,64	0,60	4,64	4,65	1,40	4,64	0,60	4,64	4,65
0,25	0,50	-10,57	10,24	-5,67	-5,54	-3,51	-3,50	1,21	0,56	1,74	0,50	0,75	3,04	0,28	3,03	2,33	0,55	2,32	0,14	2,32	2,33
	0,75	-10,73	10,09	-2,65	-2,63	-2,65	-2,62	0,33	0,39	0,30	0,79	0,46	1,87	0,10	1,87	1,19	0,21	1,19	-0,03	1,19	1,19
	1,00	-10,90	9,95	-2,65	-2,62	-0,58	-0,87	0,30	0,79	0,40	0,98	0,23	1,25	-0,02	1,25	0,46	0,03	0,46	-0,14	0,52	0,46
	0,25	-10,24	10,57	-7,07	-6,94	-7,99	-6,94	0,38	0,69	0,33	3,17	1,83	6,01	0,82	6,00	7,09	2,24	7,09	1,01	7,01	7,09
0,50	0,50	-10,40	10,40	-6,51	-6,35	-6,51	-6,35	0,31	0,57	0,31	0,57	1,11	4,07	0,45	4,06	4,07	1,11	4,07	0,45	4,06	4,07
	0,75	-10,56	10,24	-3,57	-3,61	-2,65	-2,63	1,65	0,52	0,33	0,39	0,61	2,55	0,19	2,54	1,87	0,46	1,87	0,10	1,86	1,87
	1,00	-10,72	10,10	-2,65	-2,62	-2,65	-2,62	0,33	0,51	0,30	0,79	0,34	1,57	0,04	1,57	0,99	0,15	0,99	-0,06	0,99	0,99
b/L=0,25																					
	0,25	-10,58	10,23	-5,73	-5,52	-3,50	-3,39	1,22	0,94	1,83	1,01	0,71	3,37	0,27	3,37	3,38	0,45	2,32	0,15	2,32	2,33
0,00	0,50	-10,75	10,07	-3,50	-3,39	-2,59	-2,49	1,83	1,01	0,52	1,56	0,45	2,35	0,15	2,34	2,35	0,19	1,27	-0,01	1,27	1,28
	0,75	-10,92	9,93	-2,59	-2,87	-0,90	-1,31	0,36	1,01	0,73	1,59	0,25	1,51	0,04	1,58	1,52	0,06	0,59	-0,11	0,62	0,62
	1,00	-11,09	9,79	-2,54	-2,49	-0,57	-0,56	0,55	1,56	0,94	1,65	0,13	0,95	-0,05	0,95	0,95	-0,05	0,22	-0,21	0,22	0,22
	0,25	-10,40	10,40	-5,93	-5,67	-5,93	-5,67	0,17	0,76	0,17	0,76	1,07	4,63	0,43	4,56	4,65	1,07	4,63	0,43	4,56	4,65
0,25	0,50	-10,57	10,24	-5,43	-5,12	-3,50	-3,39	1,22	0,92	1,83	1,01	0,63	3,03	0,23	3,03	2,33	0,45	2,32	0,14	2,32	2,33
	0,75	-10,73	10,09	-2,61	-2,56	-2,59	-2,49	0,41	1,02	0,52	1,56	0,36	1,86	0,10	1,86	1,19	0,18	1,19	-0,02	1,19	1,19
	1,00	-10,90	9,95	-2,59	-2,49	-0,57	-0,87	0,52	1,56	0,76	1,59	0,19	1,25	-0,01	1,25	0,46	0,04	0,46	-0,13	0,51	0,46
	0,25	-10,24	10,57	-6,83	-6,65	-7,81	-6,65	0,23	0,98	0,36	1,72	1,39	5,99	0,61	5,99	7,09	1,68	7,00	0,79	6,99	7,09
0,50	0,50	-10,40	10,40	-6,15	-6,15	-6,15	-6,15	0,13	0,71	0,13	0,71	0,87	4,06	0,34	4,05	4,07	0,87	4,06	0,34	4,05	4,07
	0,75	-10,56	10,24	-3,50	-3,39	-2,61	-2,56	1,74	1,01	0,41	1,02	0,51	2,54	0,18	2,54	1,87	0,36	1,86	0,10	1,86	1,87
	1,00	-10,72	10,10	-2,61	-2,87	-2,54	-2,49	0,41	1,01	0,55	1,56	0,26	1,57	0,05	1,64	0,99	0,14	0,99	-0,05	0,98	0,99

Table B.2—Destributed load on the centerline of slab.

L=B=8,0m

Thickness=20cm

Ec=32,0GPa

fct=1,95MPa

ks=55,0MN/m^3

T_{ev}=1.3C/cm

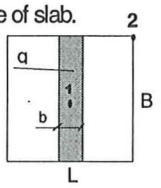

b/L=0,25																						
				MMin (kNm/m)				MMax (kNm/m)				Def. (mm)										
Reinf.		crack moment		Gamma 30 %		Gamma 60 %		Gamma 30 %		Gamma 60 %		Gamma 30 %					gamma 60 %					
p	p'	Mcr(-)	Mcr(+)	q (kN/m^2)																		
(%)	(%)	(kNm/m)	(kNm/m)	15	30	15	30	15	30	15	30	15		30		unloaded	15		30		unloaded
												2	1	2	1	2	2	1	2	1	2
	0,25	-10,58	10,23	-3,64	-3,05	-3,64	-2,37	0,63	0,88	0,63	0,78	3,39	-0,34	3,57	-0,57	3,38	2,40	-0,33	2,55	-0,56	2,33
0,00	0,50	-10,75	10,07	-3,64	-2,37	-1,99	-1,56	0,63	0,78	0,53	1,33	2,43	-0,33	2,58	-0,56	2,35	1,39	-0,31	1,53	-0,54	1,28
	0,75	-10,92	9,93	-2,45	-2,22	-1,22	-0,98	0,60	0,79	0,74	1,46	1,66	-0,32	1,81	-0,55	1,52	0,70	-0,31	0,81	-0,54	0,62
	1,00	-11,09	9,79	-1,59	-1,56	-0,57	-0,45	0,43	1,33	0,90	1,64	1,05	-0,31	1,19	-0,54	0,95	0,26	-0,31	0,31	-0,54	0,22
	0,25	-10,40	10,40	-4,69	-4,32	-4,69	-4,32	0,73	1,01	0,73	1,01	4,67	-0,36	4,84	-0,59	4,65	4,67	-0,36	4,84	-0,59	4,65
0,25	0,50	-10,57	10,24	-3,26	-2,80	-3,64	-2,37	0,57	0,84	0,63	0,78	2,99	-0,33	3,16	-0,56	2,33	2,40	-0,32	2,55	-0,56	2,33
	0,75	-10,73	10,09	-2,76	-2,74	-1,91	-1,56	0,63	0,81	0,50	1,33	2,09	-0,32	2,30	-0,55	1,19	1,30	-0,31	1,44	-0,54	1,19
	1,00	-10,90	9,95	-1,91	-1,56	-1,40	-0,81	0,50	1,33	0,74	1,61	1,37	-0,31	1,51	-0,54	0,46	0,59	-0,31	0,69	-0,54	0,46
	0,25	-10,24	10,57	-6,81	-4,99	-8,20	-4,99	0,77	0,76	0,35	0,76	5,70	-0,38	5,91	-0,62	7,09	6,70	-0,41	6,81	-0,64	7,09
0,50	0,50	-10,40	10,40	-4,69	-4,17	-4,69	-4,17	0,73	1,02	0,73	1,02	4,00	-0,35	4,15	-0,58	4,07	4,00	-0,35	4,15	-0,58	4,07
	0,75	-10,56	10,24	-3,64	-2,37	-2,76	-2,74	0,63	0,78	0,63	0,81	2,65	-0,33	2,77	-0,56	1,87	2,09	-0,32	2,30	-0,55	1,87
	1,00	-10,72	10,10	-2,48	-2,37	-1,80	-1,56	0,57	0,78	0,46	1,33	1,72	-0,32	1,88	-0,55	0,99	1,09	-0,31	1,23	-0,54	0,99
b/L=0,5																						
	0,25	-10,58	10,23	-3,85	-2,09	-2,61	-1,46	0,47	1,05	0,36	1,50	3,08	-0,40	3,20	-0,69	3,38	2,24	-0,38	2,39	-0,68	2,33
0,00	0,50	-10,75	10,07	-2,61	-1,46	-1,39	-0,52	0,36	1,50	0,61	1,80	2,26	-0,39	2,42	-0,68	2,35	1,37	-0,38	1,43	-0,67	1,28
	0,75	-10,92	9,93	-2,01	-1,16	-0,74	-0,52	0,49	1,59	0,98	1,80	1,61	-0,38	1,78	-0,67	1,52	0,76	-0,38	0,93	-0,67	0,62
	1,00	-11,09	9,79	-0,63	-0,52	-0,25	-0,42	0,92	1,80	1,04	1,85	1,02	-0,38	1,20	-0,67	0,95	0,33	-0,38	0,47	-0,67	0,22
	0,25	-10,40	10,40	-3,61	-2,09	-3,61	-2,09	0,40	1,05	0,40	1,05	4,05	-0,41	4,11	-0,70	4,65	4,05	-0,41	4,11	-0,70	4,65
0,25	0,50	-10,57	10,24	-2,69	-1,46	-2,61	-1,46	0,35	1,50	0,36	1,50	2,78	-0,39	2,95	-0,69	2,33	2,24	-0,38	2,39	-0,68	2,33
	0,75	-10,73	10,09	-2,21	-1,46	-1,03	-0,52	0,35	1,50	0,87	1,80	1,99	-0,38	2,13	-0,68	1,19	1,29	-0,38	1,37	-0,67	1,19
	1,00	-10,90	9,95	-1,39	-0,52	-0,47	-0,64	0,61	1,80	1,01	1,77	1,35	-0,38	1,41	-0,67	0,46	0,65	-0,38	0,85	-0,67	0,46
	0,25	-10,24	10,57	-4,76	-4,06	-4,49	-4,85	0,55	0,53	0,56	0,73	4,97	-0,43	4,89	-0,72	7,09	5,75	-0,44	5,57	-0,73	7,09
0,50	0,50	-10,40	10,40	-3,85	-2,09	-3,85	-2,09	0,47	1,05	0,47	1,05	3,60	-0,41	3,63	-0,70	4,07	3,60	-0,41	3,63	-0,70	4,07
	0,75	-10,56	10,24	-2,76	-1,46	-2,21	-1,46	0,33	1,50	0,35	1,50	2,44	-0,39	2,59	-0,68	1,87	1,99	-0,38	2,13	-0,68	1,87
	1,00	-10,72	10,10	-2,01	-1,16	-0,63	-0,52	0,49	1,59	0,92	1,80	1,67	-0,38	1,83	-0,67	0,99	1,05	-0,38	1,22	-0,67	0,99

Table B.3—Destributed load on the center of slab.

L=B=8,0m
Thickness=20cm
Ec=32,0GPa
fct=1,95MPa
ks=55,0MN/m^3
T_{xy}=1.3C/cm

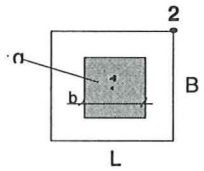

b/L=0,25																					
				MMin (kNm/m)				MMax (kNm/m)				Def. (mm)									
Reinf.		crack moment		Gamma 30 %		Gamma 60 %		Gamma 30 %		Gamma 60 %		Gamma 30 %					gamma 60 %				
p	p'	Mcr(-)	Mcr(+)	q (kN/m^2)																	
(%)	(%)	(kNm/m)	(kNm/m)	15	30	15	30	15	30	15	30	15		30		unloaded	15		30		unloaded
												2	1	2	1	2	2	1	2	1	2
	0,25	-10,58	10,23	-6,24	-6,24	-4,12	-4,11	1,77	3,37	2,01	3,61	3,46	-0,30	3,54	-0,48	3,38	2,38	-0,28	2,43	-0,46	2,33
0,00	0,50	-10,75	10,07	-4,12	-4,11	-3,02	-2,66	2,01	3,61	1,88	3,42	2,41	-0,28	2,46	-0,46	2,35	1,33	-0,27	1,32	-0,44	1,28
	0,75	-10,92	9,93	-2,66	-2,66	-1,46	-1,95	1,82	3,42	1,71	3,32	1,54	-0,27	1,55	-0,45	1,52	0,63	-0,26	0,63	-0,44	0,62
	1,00	-11,09	9,79	-2,66	-2,66	-0,82	-1,43	1,82	3,42	1,66	3,27	0,97	-0,26	0,99	-0,44	0,95	0,22	-0,26	0,22	-0,44	0,22
	0,25	-10,40	10,40	-6,24	-6,24	-6,24	-6,24	1,77	3,37	1,77	3,37	4,73	-0,33	4,81	-0,51	4,65	4,73	-0,33	4,81	-0,51	4,65
0,25	0,50	-10,57	10,24	-6,24	-6,24	-4,12	-4,11	1,77	3,37	2,01	3,61	3,13	-0,29	3,21	-0,47	2,33	2,37	-0,28	2,43	-0,46	2,33
	0,75	-10,73	10,09	-2,66	-3,55	-2,66	-2,66	1,82	3,57	1,82	3,42	1,89	-0,27	2,12	-0,45	1,19	1,21	-0,27	1,23	-0,44	1,19
	1,00	-10,90	9,95	-2,66	-2,66	-0,82	-1,71	1,82	3,42	1,66	3,32	1,28	-0,27	1,29	-0,44	0,46	0,46	-0,26	0,54	-0,44	0,46
	0,25	-10,24	10,57	-9,03	-9,30	-9,03	-9,99	1,22	2,85	1,22	2,37	6,16	-0,37	6,32	-0,55	7,09	7,25	-0,40	7,42	-0,58	7,09
0,50	0,50	-10,40	10,40	-6,91	-6,91	-6,91	-6,91	1,76	3,37	1,76	3,37	4,18	-0,32	4,28	-0,50	4,07	4,18	-0,32	4,28	-0,50	4,07
	0,75	-10,56	10,24	-4,12	-5,33	-2,66	-3,55	2,01	3,49	1,82	3,57	2,63	-0,28	2,69	-0,46	1,87	1,89	-0,27	2,12	-0,45	1,87
	1,00	-10,72	10,10	-2,66	-2,66	-2,66	-2,66	1,82	3,42	1,82	3,42	1,59	-0,27	1,61	-0,45	0,99	1,01	-0,26	1,03	-0,44	0,99
b/L=0,50																					
	0,25	-10,58	10,23	-6,07	-6,56	-4,03	-4,32	0,93	1,71	1,19	2,05	3,67	-0,43	4,03	-0,74	3,38	2,59	-0,41	2,87	-0,71	2,33
0,00	0,50	-10,75	10,07	-4,03	-4,32	-2,65	-3,11	1,19	2,05	1,03	2,01	2,62	-0,41	2,90	-0,71	2,35	1,42	-0,39	1,57	-0,70	1,28
	0,75	-10,92	9,93	-2,65	-3,81	-2,23	-3,11	1,03	2,07	1,02	2,01	1,66	-0,40	2,03	-0,70	1,52	0,72	-0,39	0,87	-0,69	0,62
	1,00	-11,09	9,79	-2,65	-3,11	-1,15	-1,85	1,03	2,01	1,09	2,21	1,10	-0,39	1,25	-0,69	0,95	0,26	-0,38	0,30	-0,68	0,22
	0,25	-10,40	10,40	-6,07	-5,90	-6,07	-5,90	0,93	1,71	0,93	1,71	4,94	-0,45	5,23	-0,76	4,65	4,94	-0,45	5,23	-0,76	4,65
0,25	0,50	-10,57	10,24	-6,74	-6,56	-4,03	-4,32	0,93	1,71	1,19	2,05	3,34	-0,42	3,65	-0,73	2,33	2,59	-0,41	2,86	-0,71	2,33
	0,75	-10,73	10,09	-3,58	-4,32	-2,65	-3,11	1,14	2,05	1,03	2,01	2,27	-0,40	2,54	-0,71	1,19	1,34	-0,39	1,49	-0,69	1,19
	1,00	-10,90	9,95	-2,65	-3,11	-1,55	-3,11	1,03	2,01	1,03	2,01	1,40	-0,39	1,55	-0,70	0,46	0,61	-0,38	0,73	-0,69	0,46
	0,25	-10,24	10,57	-7,72	-7,75	-8,90	-7,75	0,75	1,52	0,36	1,52	6,33	-0,49	6,64	-0,80	7,09	7,36	-0,52	7,66	-0,82	7,09
0,50	0,50	-10,40	10,40	-6,74	-6,56	-6,74	-6,56	0,93	1,71	0,93	1,71	4,39	-0,44	4,70	-0,75	4,07	4,39	-0,44	4,70	-0,75	4,07
	0,75	-10,56	10,24	-4,03	-4,77	-3,58	-4,32	1,19	1,97	1,14	2,05	2,84	-0,41	3,12	-0,72	1,87	2,27	-0,40	2,53	-0,71	1,87
	1,00	-10,72	10,10	-2,65	-3,81	-2,65	-3,11	1,03	2,07	1,03	2,01	1,72	-0,40	2,11	-0,70	0,99	1,14	-0,39	1,28	-0,69	0,99

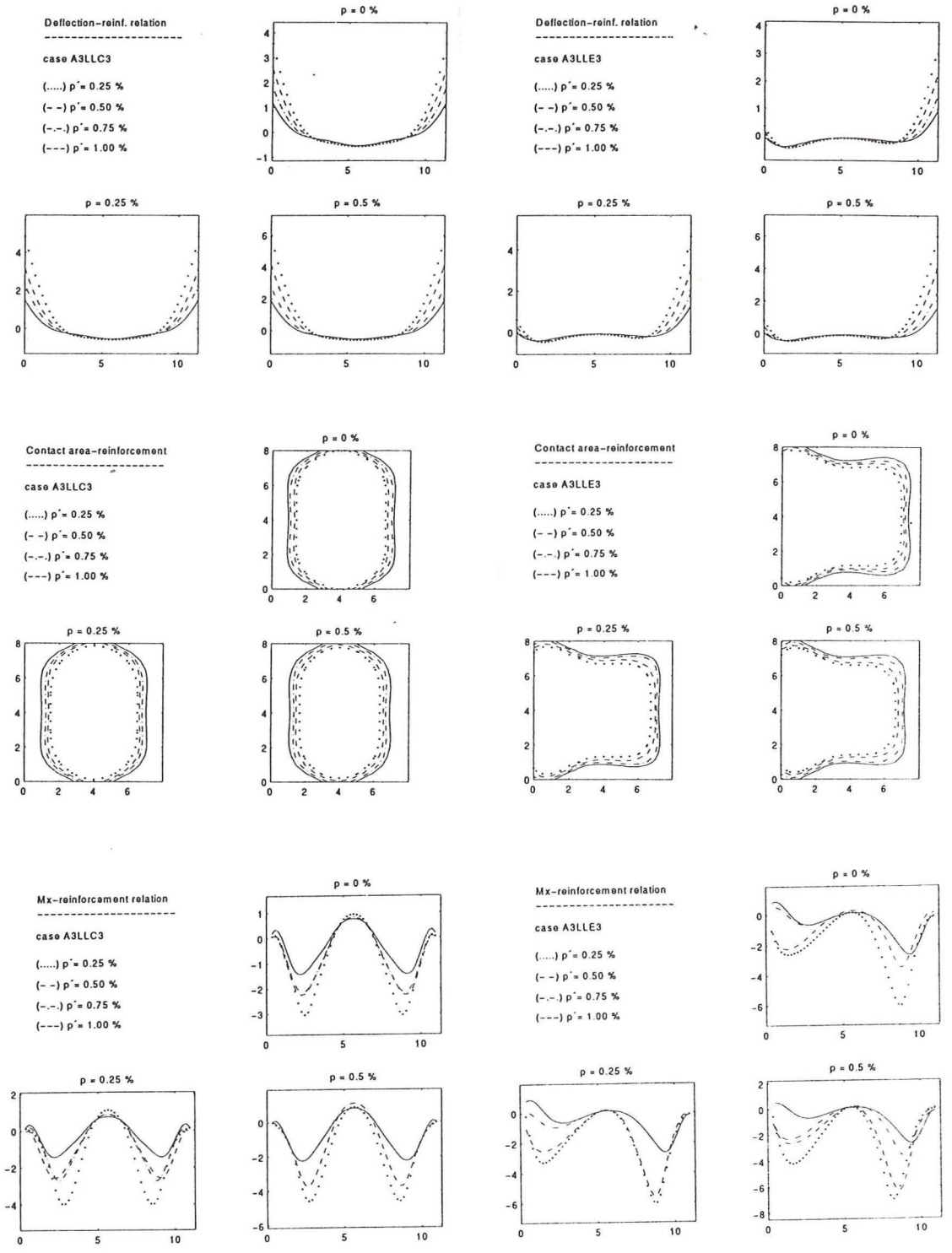

Fig. B.1 — Effect of reinforcement on corner deflection in mm(top), Contact area (middle), and Moment in kNm/m(bottom) for central- strip loading (case A3LLC3), and edge loading (case A3LLE3). $\gamma = 30$ %, t = 20 cm $E_c = 32$ GPa

References

1. ACI Committee 360, "A Preview of The Design Guide Currently Being Prepared By ACI Committee 360: Design of Slabs-on-Grade, " Concrete International: Design & Construction, V. 11 , No. 6 , June 1989, pp. 55-58.
2. Winter, G., Urquhart, L. c., and Nilson, A. H., " Design of Concrete Structures," McGraw-Hill, Inc., New York, Seventh Edition, 1964, 658 pp.
3. Abdul-Wahab, H. M. S., and Jaffer, A. S., " Warping of Reinforced Concrete Slabs Due to Shrinkage, " ACI Journal, Proceedings V. 80, Mar.- Apr. 1983, pp. 109-115.
4. Leonards, G. A., and Harr, M. E., " Analysis of Concrete Slabs on Ground," Proceeding, ASCE, V. 85, SM3, June 1959, pp. 35-58.
5. Ytterberg, R. F., "Shrinkage and Curling of Slabs on Grade: Part I — Drying Shrinkage; Part II — Warping and Curling; and Part III — Additional Suggestions," Concrete International: Design & Construction, Part I: V. 9, No. 4, Apr. 1987, pp. 22-31; Part II: V. 9, No. 5, May 1987, pp. 54-61; and Part III: V. 9, No. 6, June 1987, pp. 72- 81.
6. Sargious, M., and Wang, S. K., " Rigid Pavement Design Charts Based on a Finite Element Analysis," Roadway and Airport Pavements, SP-51, American Concrete Institute, Detroit, 1975, pp. 33-49.
7. Troxell, and Davis, "Composition and Properties of Concrete, " first edition, McGraw-Hill, Inc., 1956.
8. Branson, D. E., " Deformation of Concrete Structures," First Edition, McGraw-Hill, Inc., New York, 1977, 546 pp.
9. ACI Committee 209, " Prediction of Creep, Shrinkage, and Temperature Effect in Concrete Structures: (ACI 209R-82), " Designing for effects of creep, and shrinkage in concrete structures: Attribute to Adrian Pauw, SP-76, American Concrete Institute, Detroit, 1982, pp. 193-300.
10. Pickett, Gerald, "Shrinkage stress in concrete, " ACI Journal, Proceedings V.42, No. 3, Jan. 1946, pp. 165-204, and No. 4, Feb. 1946, pp. 361-398.
11. ACI Committee 336, "Suggested Design Procedures for Combined Footing and Mats: (ACI 336.2R-88), " ACI Structural Journal, V. 85 No. 3, May-June 1988, pp. 304- 324.
12. Bowels, J. E., "Mat Design," ACI Journal, Proceedings V. 83, No. 6, Nov. - Dec. 1986, pp. 1010 - 1017.
13. Shukla, S. N., "A Simplified method for design of mats on elastic foundation", ACI J. , Proceedings V.81, No. 5, Sept.-Oct. 1984, pp. 469-475.
14. Scanlon, A., and Murray, D. W., " Practical Calculations of Two- Way Slab Deflection, " Concrete International, V. , Nov. 1982, pp. 43-50.

15. Al-Nasra, M., and Wang, L. R. L., "Parametric Study of Slab-on-Grade Problems Due to Initial Warping and Point Loads," ACI Structural Journal, V.91 No. 2, March-April 1994, pp. 198-210.

16. Eisenmann, J., "Analysis of restrained curling stresses and temperature measurements in concrete pavements" ACI SP-25, American Concrete Institute, Detroit, 1971.

17. Schrader, E.K., " A Solution to Cracking And Stresses Caused By Dowels And Tie Bars," Concrete International, Vol. 13 No. 7, July 1991, pp. 40-45.

18. ACI Committee 302, "Guide for Concrete Floor and Slab Construction: (ACI 302.1R-80), " American Concrete Institute, Detroit, 1980, 46 pp.

19. Ritter JR, L. J., and Paquette, R. J., " Highway Engineering," Third Edition, The Roland Press Company, New York, 1967, 782 pp.

20. Boverket, Byggavdelningen, "BBK 94: Boverkets Handbok om Betongkonstruktioner, Band 1, Konstroktioner," AB Svensk Byggtjänst, Solna, 1994.

21. Ottossen, N., and Petersson, H., "Introduction to the Finite Element Method, "Printice Hall, London, 1992.

22. Thelandersson, S., " Constructionsberäkningar med Dator," Andra Upplagan, Studielitteratur, Lund, 1990, 324 pp.

23. Wang, C., and Salmon, C. G., " Third Edition, Reinforced Concrete Design," Harper & Row, New York, , 1979, 918 pp.